Received December 7, 2020, accepted December 26, 2020, date of publication January 11, 2021, date of current version January 25, 2021.

Digital Object Identifier 10.1109/ACCESS.2021.3050669

Drivers' Warning Application Through Image Notifications on the FM Radio Broadcasting Infrastructure

RADU GABRIEL BOZOMITU[1], (Member, IEEE),
FLORIN DORU HUTU[2], (Senior Member, IEEE),
AND NICOLAS DE PINHO FERREIRA[3], (Graduate Student Member, IEEE)

[1]Faculty of Electronics, Telecommunications and Information Technology, Gheorghe Asachi Technical University of Iaşi, 700050 Iaşi, Romania
[2]CITI, Inria, INSA Lyon, Université de Lyon, 69621 Villeurbanne, France
[3]Institut des Nanotechnologies de Lyon (INL), INSA-Lyon, Université de Lyon, 69621 Villeurbanne, France

Corresponding author: Radu Gabriel Bozomitu (bozomitu@etti.tuiasi.ro)

ABSTRACT In this paper a new application for transmitting image notifications on the FM radio broadcasting infrastructure, dedicated to warn drivers about significant road events and to increase the traffic safety is presented. The paper analyzes different technical solutions suitable for transmitting and receiving real-time image notifications in different scenarios by using the software-defined radio concept. In the first scenario, the image notifications are QPSK modulated and transmitted with 8 kb/s bit-rate by using a mono FM radio channel. In order to increase the speed of data transmission, the second scenario uses the FM subcarrier channels dedicated for broadcasting alternate services. In this case, a stereo FM radio channel is used to transmit data with 40 kb/s, 60 kb/s and 80 kb/s bit-rates, by using QPSK, 8-PSK and 16-PSK modulations, respectively. A new software solution to perform the real-time carrier synchronization for 8-PSK/16-PSK modulation based on a decision-directed PLL and non-linear decision block is also presented. The functionality of the proposed application was demonstrated by simulations for both transmission scenarios. Moreover, the first scenario was tested experimentally by using a professional FM transmitter and a simple RTL-SDR dongle as receiver. The customized baseband modulating signal including audio, data (image notification) and RDS signals was generated by using a device built by the authors. The receiver provides the digital signal through a USB interface to a software program, running on a processing unit, for demodulation. An experimental method for plotting the bit error rate vs. E_b/N_0 ratio, based on signal-to-noise ratio measured with a software spectrum analyzer is also proposed. This method allows the characterization of the data transmissions performed by using an experimental setup and give hints about the QPSK signal power level compared to the other ones (audio and RDS signals).

INDEX TERMS Automotive applications, digital modulation, radio broadcasting, radio communication, radio transceivers, software-defined radio.

I. INTRODUCTION

In recent years, more and more attention is being paid to the implementation of various measures to increase traffic safety for both amateur and professional drivers. This concern is motivated by the need to reduce the large number of traffic accidents that occur especially in Eastern Europe countries, particularly in Romania.

The associate editor coordinating the review of this manuscript and approving it for publication was Shadi Alawneh.

In 2019, the safest roads were in Sweden (22 deaths/million inhabitants) and Ireland (29/million), while Romania (96/million), Bulgaria (89/million) and Poland (77/million) reported the highest mortality rates. The EU average was 51 deaths per million inhabitants, according to preliminary figures released by the European Commission [1].

In Romania, the car fleet has grown enormously in the last two decades, from 3 million to 8 million vehicles. Unfortunately, at the same time, over 43,000 people have died in road accidents, the maximum being in 2008, with over 3,000 deaths, and the minimum in 2014, with

1,818 deaths [2]. Also, this is a consequence of a fact that the road infrastructure lagged behind the increase in terms of traffic. Given this negative balance, one of the priority concerns of the automotive industry from Romania has been to introduce new safety measures that will increase traffic safety.

The European Commission's Strategic Action Plan on Road Safety [3] and EU road safety policy framework 2021-2030 [4] also set out very ambitious road safety plans to reach zero road deaths by 2050 (''Vision Zero'').

Nowadays most cars are equipped with a series of safety features, such as safety-belt, airbags, antilock brakes (ABS), traction control, electronic stability control (ECS). In addition to these classic features, more and more cars are equipped by manufacturers with new safety ones, like brake assist, forward-collision warning (FCW), automatic emergency braking (AEB), pedestrian detection, adaptive cruise control, blind-spot warning (BSW), rear cross-traffic alert, lane-departure warning (LDW), lane-keeping assist (LKA), active head restraints, backup camera, parking assist systems, automatic high beams, tire-pressure monitors and others [5], [6].

In order to increase drivers' safety, different modules for the Advanced Driver Assistance System (ADAS) have been implemented in the cars [7]. ADAS systems can be grouped into several categories: adaptive, automated, for monitoring, for warning. Because many car accidents are due to driver's fatigue, the manufacturers' attention was directed to warning system, such as driver drowsiness detection [8]. In the recent years, numerous techniques have been proposed to detect driver fatigue, like steering pattern monitoring [9], vehicle position in lane monitoring [10], driver eye/face monitoring [11]–[13] and physiological measurements [14].

In this international context aiming to reduce car accidents, the focus of researchers is on developing new applications that will contribute to increase the traffic safety. Many car accidents are due to the occurrence of dangerous situations in traffic (which are not currently signaled, are due to sudden changes in weather, or are due to an inappropriate infrastructure) for which drivers are not prepared to react or they are reacting too slowly. Early signaling of dangerous traffic events by using a radio communications system will increase traffic safety and will significantly reduce road accidents with victims.

Different types of radio access technologies, such as cellular vehicle-to-everything (C-V2X) and dedicated short-range communication (DSRC) are used to implement vehicular networks for robust communications between vehicles. By using these communication technologies many applications like road traffic safety and infotainment related services developed within new intelligent transportation systems (ITS) can be implemented. DSRC and C-V2X are technologies used for very high-speed and high-frequency data exchange, and require extensive and very expensive infrastructure deployment. Both DSRC and C-V2X use the same message sets and use cases and the 5.9 GHz band to directly communicate from one radio to another. DSRC uses Wireless Access in Vehicular Environments (WAVE) protocol stack, while C-V2X uses 4G long-term evolution (LTE) or 5G mobile cellular connectivity. As a result, a DSRC radio cannot talk to a C-V2X radio, and vice versa. The range of DSRC is typically 300m, while C-V2X may have 20-30% more range than DSRC as well as significant performance improvement related to communication obstructions. In addition to the direct communication (V2V, V2I), C-V2X also supports wide area communication over a cellular network (V2N). One of the major impediments of wireless communication systems is their limited capacity (limited number of channels and limited data rates). In order to take advantage of both access technologies, they should be integrated together in intelligent vehicles. At present, C-V2X is not mature yet, while DSRC has some drawbacks like small coverage and low throughout, which makes them unsuitable for certain types of applications.

This paper proposes a new and easy to implement technical solution for real-time warning of potentially dangerous traffic situations, without distracting the driver, by transmitting real-time image notifications via FM radio broadcasting. By using this technology, it is possible to perform robust one-way long-range communication scenarios at a much lower cost than in the case of other communication technologies. Moreover, this technology allows an unlimited number of users. In order not to distract the driver, the graphic part of the application is simplistic, containing less information than in the case of GPS-based navigation applications, used by most cars today. The advantages of using FM transmissions are that the FM infrastructure is extremely widespread, has a large coverage area (especially for areas where the Internet signal is very weak or not present at all) and ensures a good enough transmission quality.

According to the Romanian Government Decision (HG from 14.09.2018) for the approval of the ''Strategy on the implementation of digital terrestrial sound broadcasting and associated multimedia services, at national level'', published on the website of the Ministry of Communications and Information Society, in Romania, the transition from analog to digital audio broadcasting (DAB) radio, which offers services for data transmissions, will take place between 2025-2027. This paper proposes an immediate alternative technical solution to transmit data on FM radio broadcasting for the implementation of a real-time driver warning application.

Several techniques for data transmission on FM radio are reported in the literature [15]–[20]. In [15] a simple solution is presented for transmitting data in FM signal with only 3 kb/s bit-rate by using the On-Off Keying (OOK) modulation scheme onto a 12 kHz carrier and multiplexed with an audio signal. In [16] the Multi Purpose Radio Communication Channel (MPRC) technology is used to deliver data at maximum data rate of around 40 kb/s by using a proprietary codec algorithm: Subsidiary Communication Channel (SCC). In [17] the implementation of a Subsidiary Communications Authorization (SCA) system used for text transmission on

broadcasting system by using FSK modulation is presented. The baud rate of delivery and data acceptance provided by this system is equal to 600 bps. In [18] the discrete wavelet transform (DWT) technology is used to improve the video compression level in order to store and to transmit the video signal at 16 kb/s through any reliable media with a reasonable video quality. In [19] a method of transmitting stationary TV pictures within the bandwidth of an FM subsidiary communications authorization subchannel and using conventional cameras and monitors is discussed.

The West-European standard of FM transmission uses the frequency band of 87.5–108 MHz with a frequency deviation of 75 kHz. The total signal frequency band for CCIR standard in mono mode is 180 kHz, while in stereo mode it is 256 kHz. The frequency grid is dividable to 100 kHz [20].

In the recent years, systems for the additional transmission of data on additional subcarriers have been used [20]. Thus, the following data transmissions are allowed: the broadcast channel multiplexing system UVK2 (with two subcarriers 46.875 kHz and 78.125 kHz); data transmission system RDS (Radio Data System) on a 57 kHz subcarrier (third harmonic of the pilot-tone); the road data transmission system ARI (''Autofahrer Rundfunk Data''), also on a 57 kHz subcarrier, possible together with RDS; the additional data transmission SCA system on a 67 kHz subcarrier (in other countries on 92 kHz) which uses the frequency modulation with 6 kHz deviation and the additional signal frequency band is 30–6000 Hz [20]. In 1997, in addition to RDS, the system of 16 kbit/s bit-rate data transmission DARC (Data Radio Channel) on 76 kHz subcarrier (fourth pilot-tone harmonic) has been introduced [20], [21].

The Federal Communications Commission (FCC) established the policy statement for transmission in Broadcast Radio Subcarriers, which represents a data channel that is transmitted along with the main audio signal over a broadcast station. Subcarriers are used for many different purposes, including (but not limited to) paging, inventory distribution, bus dispatching, stock market reports, traffic control signal switching, point-to-point or multipoint messages, foreign language programming, radio reading services, according to Policy Statement adopted by the Federal Communication Commission no. 22 Record [22]. According to this document, during monophonic program transmissions, multiplex subcarriers and their significant sidebands must be within the 20 kHz to 99 kHz range; during stereophonic transmissions, their range is restricted between 53 kHz and 99 kHz [22].

Because the subcarrier channels are not receivable with a regular radio, in this paper we developed special software-defined radio (SDR) receivers, which are able to receive image notifications on the FM radio broadcasting. Due to its flexibility, adaptability and programmability, the SDR receiver can adapt easily to various air standards and waveforms, frequency bands, bandwidths, and operating modes [23]–[26]. Moreover, the bandwidth employed for FM transmission is narrow, less than 100 kHz, consequently, the SDR provides a reliable solution without a high computational cost.

The drivers' warning application proposed in this paper includes two data transmission scenarios with different speeds and by using different digital modulation types – QPSK, 8-PSK and 16-PSK [27]–[30] on the FM radio broadcasting: (1) low speed data transmission on the mono FM radio channel by using QPSK modulation on a 11 kHz subcarrier with 8kb/s bit-rate; (2) high speed data transmission on the stereo FM radio broadcasting by using QPSK/8-PSK/16-PSK modulation types on a 76 kHz subcarrier with 40 kb/s, 60 kb/s and 80 kb/s bit-rate, respectively.

In the first scenario, the available frequency bandwidth used for data transmission is 8 kHz, while in the second scenario it is 46 kHz (53 – 99 kHz), the same as in the DARC standard, but using different types of digital modulation to increase the data transmission speed. The first scenario was tested experimentally in the laboratory conditions by using a device built by the authors to generate the customized baseband signal used as a modulating signal for a professional FM radio transmitter. In this case, the baseband signal includes the QPSK data signal onto a 11 kHz carrier, multiplexed with an audio mono signal having a bandwidth of 5 kHz and the RDS signal used to transmit warning notifications as a text message.

For the second scenario, which was tested by simulations in MathWorks' Matlab-Simulink software, the customized baseband signal contains the FM radio multiplex (MPX) signal and the digital modulated data signal onto FM subcarrier channel of 76 kHz. In this case, the customized baseband FM signal transmitted on an additive white gaussian noise (AWGN) communication channel is software generated. The receiver is implemented based on SDR concept, by using a cheap RTL-SDR device, which provides the digital baseband FM signal through a USB interface to a Simulink-based FM receiver. The received signal is non-coherently demodulated using a Complex Delay Line Frequency Discriminator (CDLFD) and the data signal is recovered by using a carrier synchronization loop based on decision-directed phase-locked loop (PLL).

The performances of the data transmissions are analyzed by plotting the bit error rate (BER) depending on E_b/N_0 ratio for all transmission scenarios.

The rest of the paper is organized as follows. Section 2 provides a description of the proposed drivers' warning application. It presents also the implementation of different types of software-defined radio communication systems for image notifications transmitted with different speed on the usual FM radio broadcasting. Section 3 shows the simulation results for all transmission scenarios analyzed in the paper, a new method for signal-to-noise ratio (SNR) measurement by using a software spectrum analyzer and presents the results experimentally obtained for the case of transmitting image notifications on the mono FM radio broadcasting. Section 4 outlines the

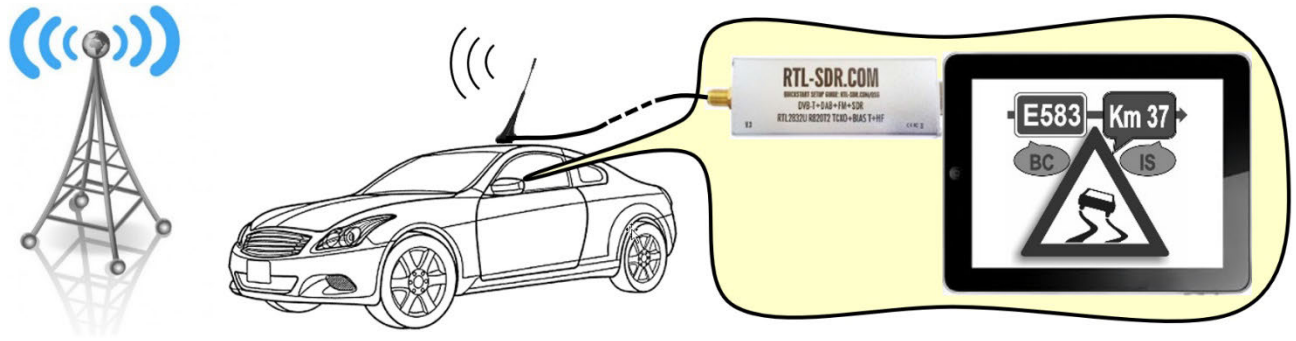

FIGURE 1. Driver warning by image notifications sent on FM radio broadcasting.

conclusions of this paper and gives some future directions for this work.

II. MATERIALS AND METHODS

A. DESCRIPTION OF THE PROPOSED DRIVERS' WARNING APPLICATION

The proposed application warns drivers in real-time by sending an image notification about an important traffic event. The image notification is sent on the FM radio together with the usual radio broadcasting, according to the block diagram illustrated in Fig. 1. Compared to the Radio Data System Traffic Message Channel (RDS-TMC) [31], which warns drivers through text messages that may be difficult to read without distracting them, the proposed system uses pictograms, with a greater visual impact and which are easier to understand by drivers.

The structure of the application includes an FM broadcasting station, which transmits the image notifications, the driver receiving device represented by a simple Tablet PC (currently used by many cars) and an RTL-SDR device connected to the car antenna and USB connected to the Tablet PC (Fig. 1). The software component of the driver's device includes the software-defined radio receiver, which is able to receive both image notifications and the FM broadcasting at the same time.

The database of images for traffic events notifications is represented by black and white images of small dimensions (100×100 pixels). Some examples are illustrated in Fig. 2. An image notification represents the road identification (ex. A2, DN1, E583), the location of the traffic event on the public road (kilometric point on the road where the traffic event occurs) and a simple image representation of a traffic event. The database of image notifications is updated in real-time depending on the traffic events announced by the road authorities and may contain classic traffic signs also.

The data transmission speed achievable by the system is high enough for the proper operation of the drivers' warning application by real-time transmitting of image notifications.

Two types of applications for transmitting image notifications on the FM broadcasting can be implemented. First, one way to implement the notification system is based on a national standard FM radio broadcasting infrastructure. This infrastructure is covering the public roads or a highway by FM radio stations to signal different unexpected events that may occur in traffic. In this case, due to the diversity of traffic event types, as well as the locations where they can occur, the image notifications are built at the transmitter stage, according to the traffic events reported by the road authority.

Second, another way to implement the notification system is by using low power radio FM transmitters to signal in advance (few tenths of meters), by both image notifications and audio signals, planned traffic events. For example, these traffic events may be: railway crossing passes, traffic lights, pedestrian crossing, dangerous intersections, etc. Statistics have demonstrated that in Romania, many car accidents occur when crossing the railway. This latter application can be implemented by using the first transmission scenario presented in the paper (i.e., pictogram transmission using QPSK modulation). In this case both the audio signal (used for driver warning by sound) and image notification (used for driver warning by image notification) occupying a bandwidth of 15 kHz are transmitted simultaneously on the mono FM radio. Thus, drivers are warned (by image notification and sound) in advance about traffic events that require a quick reaction from them, even in situations of great fatigue. The proposed solution may be implemented rapidly, with low-cost infrastructure and with minimum modifications on the receiver side also.

A similar technique is currently employed by some cars for detection and recognition of the road traffic signs through image recognition. Its drawback is that they are signaled from a short distance and may not even be recognized by the application in the case of damaged traffic signs or when the visibility is low due to bad weather or during the night time. Moreover, this technique based on image recognition uses machine learning based classification algorithm, such as Artificial Neural Networks (ANN) and Support Vector Machines (SVM), requiring high processing power. On the other hand, our proposed application solves these problems contributing to increase traffic safety.

In the latter scenario case, in order to increase the speed of the data transmission, only the traffic event code (in the form

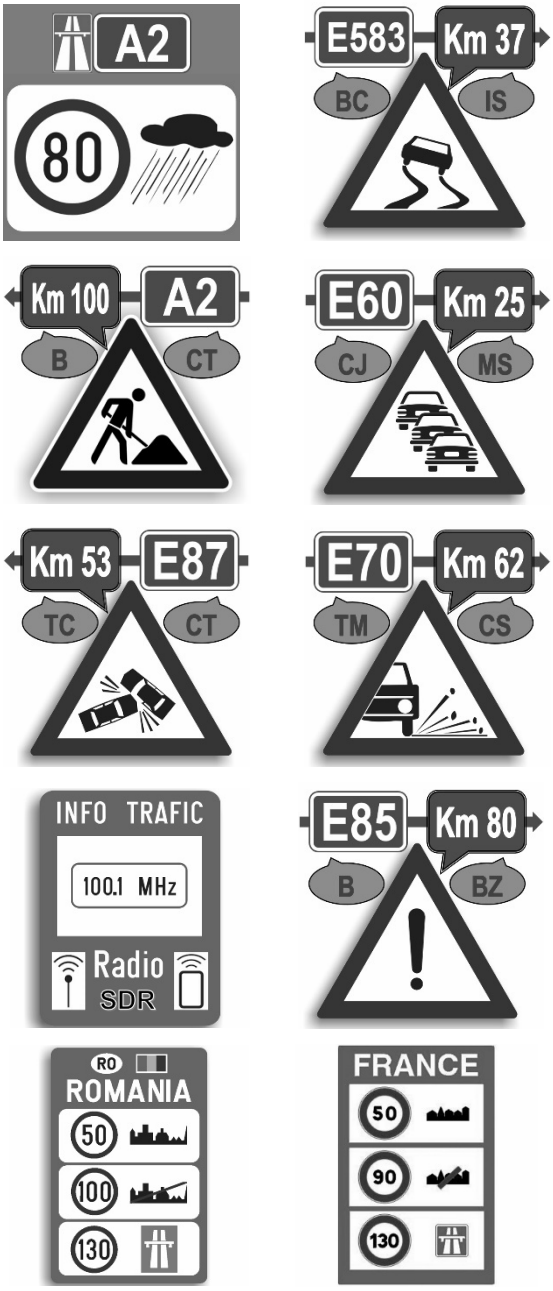

FIGURE 2. Examples of image notifications used by the proposed drivers' warning application.

of a text message) can be transmitted. Therefore, the image notifications are built into software at the receiver stage, according to the received code, by using different images form the local database of the application.

B. TRANSMISSION OF IMAGE NOTIFICATIONS ON THE FM BROADCASTING BY USING SOFTWARE-DEFINED RADIO COMMUNICATION SYSTEMS

The principle of image transmission via FM radio broadcasting is illustrated in Fig. 3. A customized baseband signal (containing both data and audio signals) software generated by Matlab – Simulink program is used as modulating signal for a professional FM transmitter.

The transmitted FM signal is received by using a simple RTL-SDR dongle (commercially available at a low price), which provides the baseband FM modulated signal to the software program. This signal is demodulated with a software-defined FM radio receiver in order to extract the image notification in the same time with the usual FM broadcasting.

1) TRANSMISSION AND RECEPTION OF IMAGE NOTIFICATIONS ON THE MONO FM RADIO BROADCASTING

A simple method to transmit data on FM radio broadcasting consists of using a mono FM transmitter, according to the method illustrated in [15].

In Fig. 4 the block diagram used to create the customized baseband signal for mono FM transmission is illustrated. Although this signal contains a QPSK data signal, it represents the modulator signal for a classic mono FM transmitter. For the simulation setup, the baseband FM signal is generated by using a DC carrier frequency modulated by the information signal, $s_i(t)$, according to the block diagram illustrated in Fig. 5 [15]. This stage represents a voltage-controlled oscillator (VCO) with the sensitivity $k_0 = 2\pi K_{fm}$ (Hz/V), representing the FM modulation constant.

According to the block diagram illustrated in Fig. 5, the baseband FM signal can be expressed as follows:

$$s_{bb\_fm}(t) = A_c \cos\left(0 + 2\pi K_{fm} \int_0^t s_i(t)dt\right) \tag{1}$$

where A_c is the magnitude of the baseband FM signal.

For practical implementation of this transmission scenario, the customized baseband signal is generated by using a device implemented by authors, presented in detail in Section 3. In this case, the spectrum of the customized baseband signal (illustrated in Fig. 6) includes the audio signal, band-limited to 5 kHz, the QPSK data signal onto a 11 kHz carrier (software generated as it is shown in Fig. 4) and the RDS signal onto a carrier frequency of 57 kHz used to transmit simplified waring notifications as a text message for the standard car receivers. The available frequency bandwidth used to transmit information data is equal to 8 kHz and the transmission bit-rate has been established to 8 kb/s.

The customized baseband signal for mono FM transmission can be expressed as follows:

$$\begin{aligned} s_{i\_mono\_fm}(t) = {} & s_{audio}(t) + s_{I\_QPSK}(t) \cdot \cos(2\pi f_{11k} t) \\ & + s_{Q\_QPSK}(t) \cdot \sin(2\pi f_{11k} t) + s_{rds}(t) \end{aligned} \tag{2}$$

where $s_{audio}(t)$ is the audio signal, $s_{I\_QPSK}(t)$ and $s_{Q\_QPSK}(t)$ are the real part and the imaginary part of the baseband QPSK signal and $s_{rds}(t)$ is the RDS signal. The $s_{rds}(t)$ signal onto a carrier frequency of 57kHz can be written:

$$s_{rds}(t) = s_{bb\_rds}(t) \cdot \cos(2\pi f_{57k} t) \tag{3}$$

where $s_{bb\_rds}(t)$ is the baseband RDS signal.

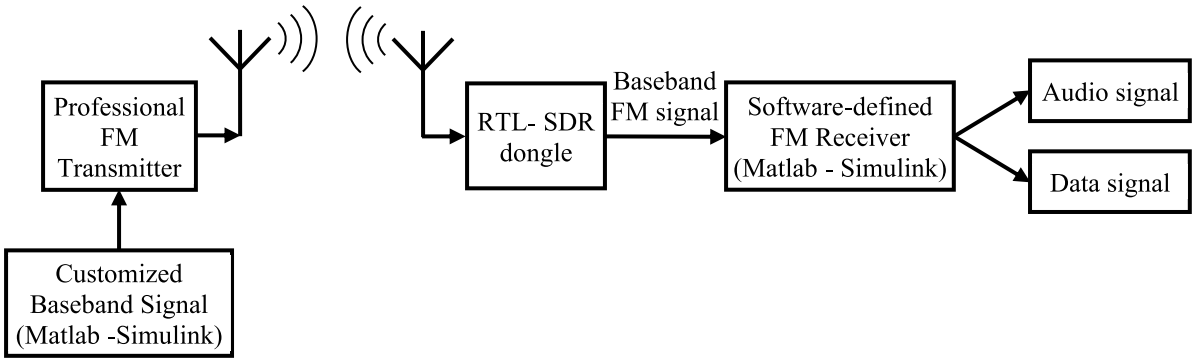

FIGURE 3. Wireless transmission of image notifications on the FM radio broadcasting.

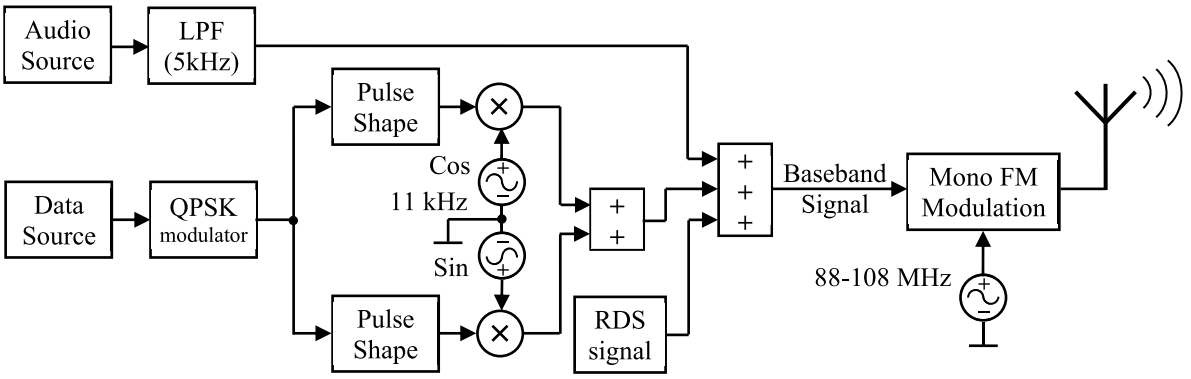

FIGURE 4. Creating the customized baseband signal for mono FM transmission.

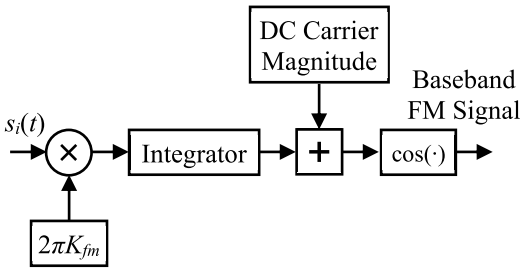

FIGURE 5. Baseband FM signal generator.

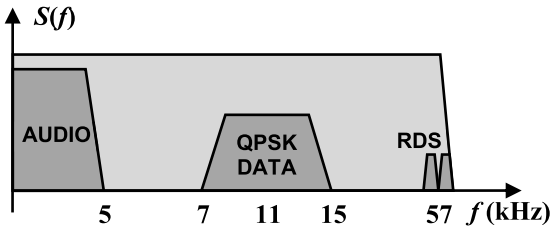

FIGURE 6. Spectrum of the customized baseband signal used to transmit information data by using a mono FM transmission.

Although this method can only be used for mono FM transmissions, it is very simple and easy to implement on any type of FM transmitter because it does not require hardware modifications of the transmitter. As stated, at the receiver side, the modifications are minor, only an RTL-SDR receiver, at least for the existing car park.

In Fig. 7 the block diagram of the Simulink-based mono FM radio receiver is presented. The received baseband FM signal is non-coherently demodulated using a CDLFD [15]. According to the FM transmission, the demodulated signal is then processed by using a de-emphasis block. The audio signal corresponding to the mono FM radio broadcasting and QPSK modulated data (used for image notifications) onto 11 kHz carrier frequency are separated from each other by using a "low-pass" infinite impulse response (IIR) filter with a 5 kHz cut-off frequency and an 8 kHz "band-pass" finite impulse response (FIR) filter, respectively.

In order to extract the image notification, the QPSK data signal is demodulated by using a carrier synchronization loop operating at baseband, as it is illustrated in [15]. The image reconstruction stage for data transmission with 8 kb/s bit-rate is based on a procedure illustrated in [15]. A RDS signal demodulator is used to extract supplementary text message notifications, which can also be received by conventional FM receivers, used by cars which are not equipped with a Tablet PC for running the software defined radio receiver. This transmission scenario has been analyzed both by simulation and practically in laboratory conditions, according to the principle illustrated in Fig. 3. The simulation and experimentally obtained results are presented in Section 3.

2) TRANSMISSION AND RECEPTION OF IMAGE NOTIFICATIONS ON THE STEREO FM RADIO BROADCASTING

The method illustrated principally in Fig. 3 can also be used for data transmission on the stereo FM radio broadcasting.

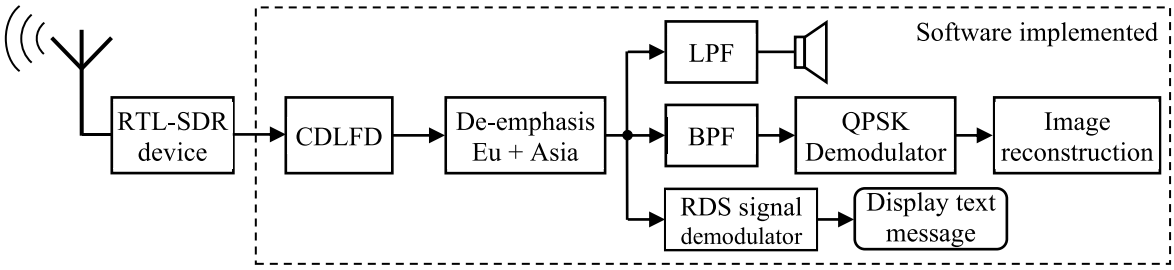

FIGURE 7. Block diagram of the Simulink-based mono FM radio receiver.

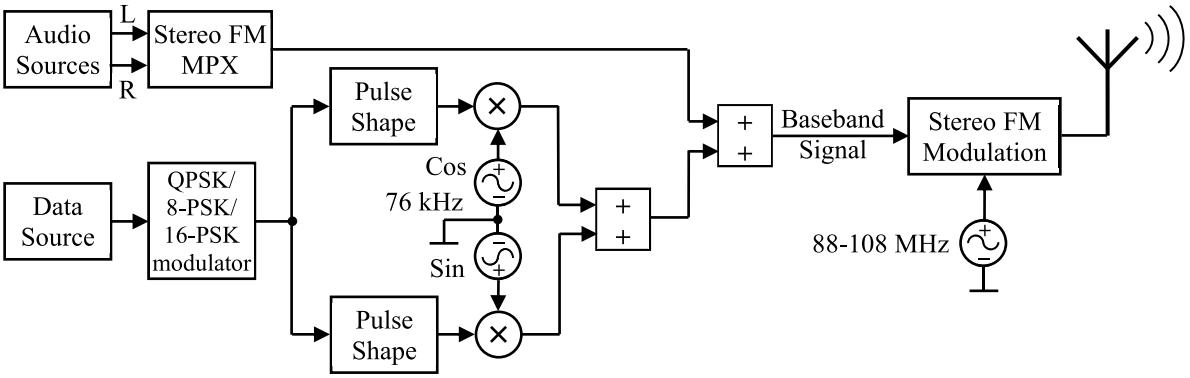

FIGURE 8. Creating the customized baseband signal for stereo FM transmission.

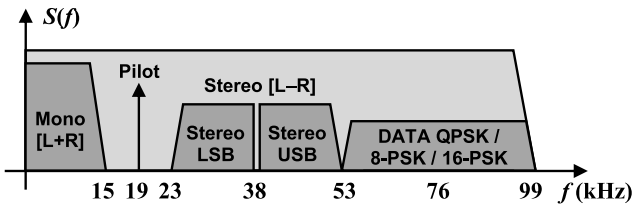

FIGURE 9. Spectrum of the customized MPX signal used to transmit information data by using a usual stereo FM transmission.

In this case, in order to increase the bit-rate, the data transmission is performed in the FM Broadcast Radio Subcarriers Channel by using a subcarrier on a frequency of 76 kHz. The block diagram used to create customized baseband signal for stereo FM transmission is illustrated in Fig. 8. The spectrum of the customized baseband signal (illustrated in Fig. 9) includes the stereo multiplex signal and the information data signal onto a 76 kHz carrier. Depending on the application type, the information data signal is QPSK, 8-PSK and 16-PSK modulated onto a 76 kHz carrier and the transmission bit-rate has been established to 40 kb/s, 60 kb/s and 80 kb/s, respectively. This requires an available frequency bandwidth of 40 kHz around the carrier, for all modulation types.

The customized baseband signal for stereo FM transmission can be expressed as follows:

$$s_{i\_stereo\_fm}(t) = s_{mpx}(t) + s_{I\_M-PSK}(t) \cdot \cos(2\pi f_{76k} t) + s_{Q\_M-PSK}(t) \cdot \sin(2\pi f_{76k} t) \quad (4)$$

where $s_{mpx}(t)$ is the FM radio multiplex signal, $s_{I\_M-PSK}(t)$ and $s_{Q\_M-PSK}(t)$ are the real part and the imaginary part of the baseband M-ary PSK (M-PSK) signal ($M = 4, 8, 16$).

The implementation of this technique requires hardware modification of the transmitter by extending the spectrum of the MPX signal and by adding a new spectral component on the carrier frequency of 76 kHz in the FM Broadcast Radio Subcarriers Channel.

In Fig. 10 the block diagram of the Simulink-based stereo FM radio receiver is presented.

This receiver, similar to the one implemented in [15] consists of the same non-coherent demodulator stage based on CDLFD, a stereo FM demultiplexer, a stereo decoder stage, a de-emphasis stage, a 40 kHz "band-pass" FIR filters used to select the QPSK/8-PSK/16-PSK modulated signal transmitted onto a 76 kHz carrier frequency and an image reconstruction stage for data transmission with 40 kb/s, 60 kb/s and 80 kb/s bit-rates, respectively. The information data (corresponding to image notifications) is extracted by using the demodulation principle based on a decision directed PLL illustrated in [15], but using a new software implementation of a synchronization loop for demodulation of QPSK, 8-PSK and 16-PSK signals onto a 76 kHz carrier. The software implementation of this synchronization loop is illustrated in detail in the next Subsection. This transmission scenarios have been analyzed only by simulation according to the principle illustrated in Fig. 3 and the obtained results are presented in Section 3.

3) A NOVEL IMPLEMENTATION OF A SYNCHRONIZATION LOOP BASED ON A DECISION DIRECTED PLL FOR QPSK/8-PSK/16-PSK SIGNAL DEMODULATION

In Fig. 11 a synchronization loop for QPSK/8-PSK/16-PSK signal demodulation, based on a decision-directed PLL

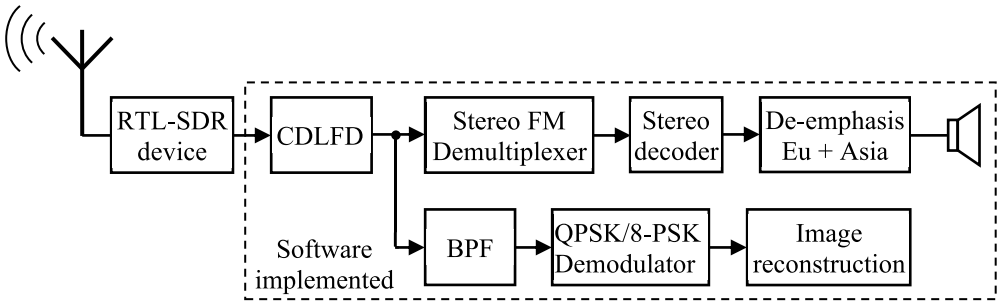

FIGURE 10. Block diagram of the Simulink-based stereo FM radio receiver.

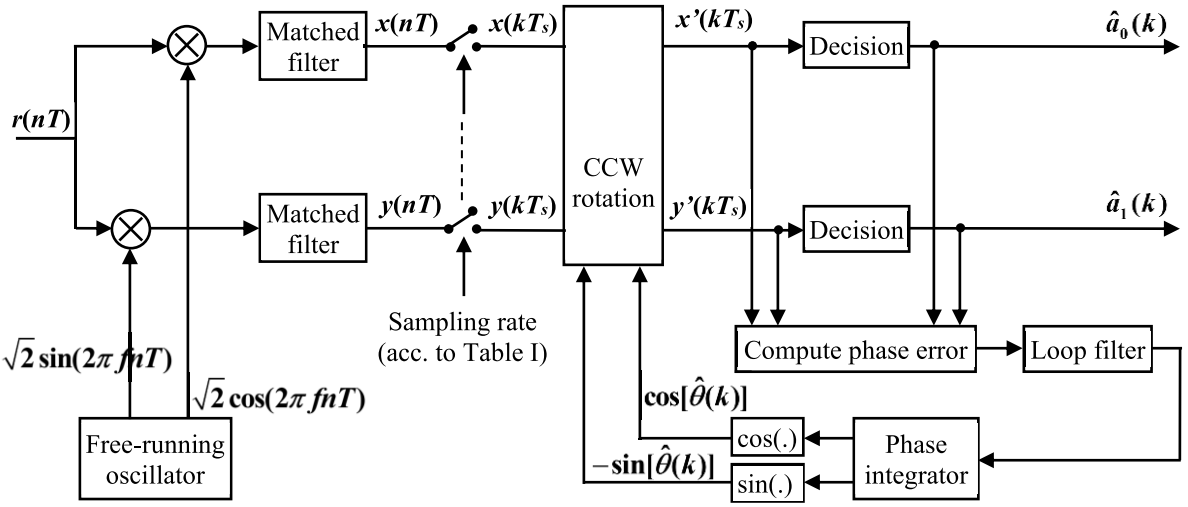

FIGURE 11. Carrier synchronization loop based on decision-directed PLL and non-linear decision block [15].

and non-linear decision block is presented [15]. Compared to other implementations, based on carrier synchronization at the demodulation stage [15], or by using Mth-power loop [32], this system achieves carrier synchronization by operating at the symbol samples and thus requires less processing power being suitable for real-time applications.

The decision block uses symbol estimates to compute phase error as the difference between the two phases and can be written [15]:

$$\theta_e(k) = \theta_r(k) - \theta_s(k) \tag{5}$$

where

$$\theta_s = \tan^{-1}\left[\frac{\hat{a}_1(k)}{\hat{a}_0(k)}\right]; \quad \theta_r = \tan^{-1}\left[\frac{y(kT_s)}{x(kT_s)}\right] \tag{6}$$

In (6), $\hat{a}_0$ and $\hat{a}_1$ represent the IQ estimated symbol values.

The demodulation is performed with a fixed frequency quadrature oscillator as shown in Fig. 11 (at 11 kHz and 76 kHz frequencies for the first and second transmission scenarios, respectively), and then a subsequent frequency correction at baseband is performed by the synchronization loop. Continuous rotation of the constellation points due to the residual frequency offset is compensated by the synchronization loop, which perform ''de-rotation'' of the constellation to its desired position. To improve synchronization, the sampling rate used by the carrier synchronization loop illustrated in Fig. 11 is chosen as multiple of the input data rate for all types of digital modulations used by the proposed application.

For QPSK signal demodulation, the decision block in Fig. 11 is represented by simple hard limiters, implemented with *sign* function. For 8-PSK and 16-PSK demodulation, the decision block is represented by multivalued limiters with 4 or 8 positive and negative values, respectively and nonuniform steps. For M-PSK signals, this nonlinearity function, $F(x)$, is given by the following equation [33]:

$$F(x) = \sin\left[\frac{(2l-1)\pi}{M}\right] \tag{7}$$

where $l = 1, \cdots, L; L = M/4$.

The decision level can be calculated according to the following equation [33]:

$$\delta_l = \begin{cases} 0, & l = 1 \\ \sin\dfrac{2(l-1)\pi}{M}, & 2 \le l \le \dfrac{M}{4} \\ \infty, & l > \dfrac{M}{4} \end{cases} \tag{8}$$

TABLE 1. Parameters of all transmission scenarios.

FM transmission	Digital modulation type	Bit-rate (kb/s)	Symbol-rate (kb/s)	Sampling rate (kHz)	No. of bits per symbol	Carrier frequency (kHz)	f_i (kHz)	$2\pi K_{fm}$ (Hz/V)	Available frequency bandwidth (kHz)	Image processing time (sec)
Mono FM	QPSK	8	4	288	72	11	15	4	8	12.849
Stereo FM	QPSK	40	20	480	24	76	96	3	46	2.569
	8-PSK	60	20	480	24	76	96	3	46	1.747
	16-PSK	80	20	480	24	76	96	3	46	1.322

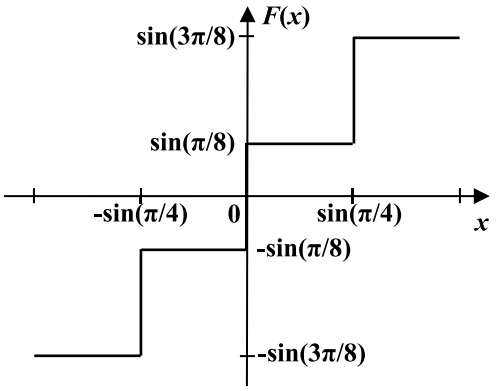

FIGURE 12. 8-PSK loop nonlinearity.

In Fig. 12 the function $F(x)$ is customized for the case of 8-PSK modulation. Thus, according to (8) and Fig. 12, the decision levels for 8-PSK modulation are 0 and $\pm\sin(\pi/4)$; for 16-PSK modulation, these levels are: 0, $\pm\sin(\pi/8)$, $\pm\sin(\pi/4)$, $\pm\sin(3\pi/8)$.

According to the definition of function $F(x)$ in Fig. 12, for proper operation of the multilevel limiter loop, its argument must be normalized. This is done by using an AGC in the 8-PSK/16-PSK loop in order to provide correct data estimates for all eight/sixteen quadrants in the constellation diagram.

III. RESULTS

The performances of the proposed drivers' warning application were analyzed by simulation, but also experimentally in laboratory conditions for the case of mono FM radio transmission.

A. SYSTEM TESTING BY SIMULATION

The operation of all transmission scenarios proposed in the paper is first analyzed by using the simulation setup illustrated in Fig. 13, that was built in Matlab-Simulink. In this case both the transmitter and receiver are software implemented and the generated baseband FM signal is transmitted on an AWGN communication channel. The block diagrams of the software-defined mono FM transmitter and receiver circuits employed in our analysis are illustrated in Figs. 4 and 7, respectively and the block diagrams of the software-defined stereo FM transmitter and receiver circuits are presented in Figs. 8 and 10, respectively.

The frequency deviation employed by the proposed system is the one used by commercial radio FM stations, $\Delta f = 75$ kHz. Since in our application the maximum frequency of the information signal (including the audio signal and the digital modulated data signal) is $f_i = 15$ kHz/96 kHz, the bandwidth of the FM signal is $B = 180$ kHz/342 kHz for mono and stereo FM radio transmission, respectively. These characteristics are obtained by setting the parameter $2\pi K_{fm} = 4$ Hz/V/3 Hz/V for mono/stereo FM radio transmission in the FM generator stage from Fig. 5. For simplification, the RDS signal was not considered in the case of mono FM transmission analyzed by simulation, but it has been included in the experimental setup.

In Table 1 the parameters of all transmission scenarios analyzed in the paper are shown. In Fig. 14 the simulation results for the mono FM broadcasting and data transmission by using QPSK modulation with 8 kb/s bit-rate are illustrated. In Fig. 14 (a) the spectrum of the baseband FM signal is presented. Fig. 14 (b) illustrates the spectrum of the customized baseband signal used at the transmitter stage which includes the audio signal band-limited to 5 kHz and the QPSK data signal around a 11 kHz carrier. In Fig. 14 (c) the spectrum of the received QPSK data signal around a 11 kHz carrier is illustrated and in Fig. 14 (d) the spectrum of the received audio signal is represented.

In Figs. 15, 16 and 17 the same simulation results are illustrated for stereo FM transmissions including digital modulations QPSK with 40 kb/s, 8-PSK with 60 kb/s and 16-PSK with 80 kb/s, respectively.

The bit error rate of all digital transmissions included in mono and stereo FM broadcasting is calculated depending on E_b/N_0 ratio, according to the following equation [27]:

$$E_b/N_0 = (C/N) \cdot (B/f_b) \tag{9}$$

where E_b is the energy of a bit, N_0 is the thermal noise power density, C is the carrier power, f_b is the bit-rate per second, and B is the frequency bandwidth of the circuit.

For QPSK, 8-PSK and 16-PSK digital modulations, considered in the radio transmissions used by the proposed application, the ratio B/f_b in (9) is equal to 1/2, 1/3 and 1/4, respectively.

The higher the number of input data bits, the more accurate the estimation of the BER, but it requires longer simulation times, which are computationally expensive and difficult to implement. A good estimate of the BER can be obtained

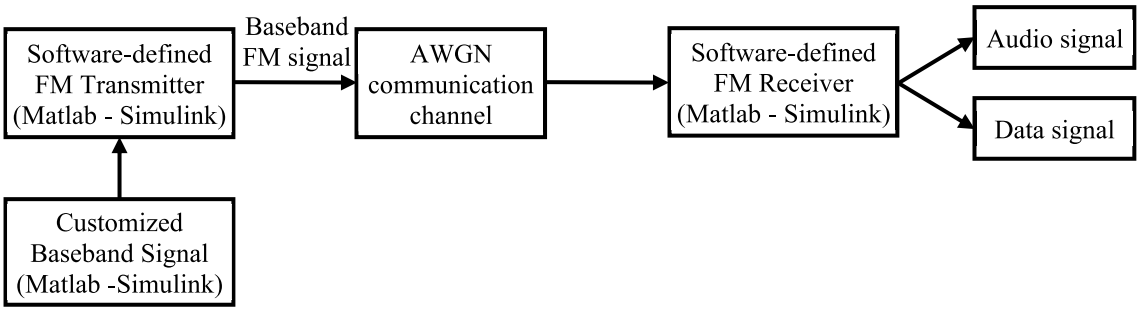

FIGURE 13. Simulated transmission of image notifications and audio signal on the AWGN communication channel.

from the simulations that provides at least 100 bit errors [27]. As a consequence, for a highly accurate estimation of the BER we consider a number of 480000 input data bits for all transmission scenarios analyzed in the paper.

In Fig. 18 the constellation diagrams of all modulations (QPSK, 8-PSK and 16-PSK) used for digital transmission performed in the proposed drivers' warning application are presented.

In Fig. 19 the bit error rate depending on E_b/N_0 for all digital transmissions (with QPSK, 8-PSK and 16-PSK modulations) analyzed in the proposed drivers' warning application are illustrated and compared with the corresponding ideal curves. The average theoretical bit error probability for M-ary PSK modulations, for M>2, over the AWGN channel is [27]:

$$\mathrm{BER} \cong \frac{1}{\log_2 M}\mathrm{erfc}\left(\sqrt{\frac{E_b \log_2 M}{N_0}}\sin\frac{\pi}{M}\right) \tag{10}$$

The simulation results show that the data transmissions of image notifications are performed without any error for E_b/N_0 ratios higher than 11 dB (for QPSK modulation implemented in both mono and stereo FM transmission), 15 dB (for 8-PSK modulation) and 20 dB (for 16-PSK modulation).

According to simulation results illustrated in Fig. 19, the lowest value of the E_b/N_0 ratio for which the image notification can still be detected (but for a low quality) is: 2 dB for QPSK modulation implemented in mono FM radio transmission; 0 dB for QPSK modulation implemented in stereo FM radio transmission; 5 dB for 8-PSK modulation; 9 dB for 16-PSK modulation.

The image notification is considered of high quality for the proposed drivers' warning application for E_b/N_0 ratios higher than: 8 dB for QPSK modulation implemented in both mono and stereo FM transmission; 11 dB for 8-PSK modulation and 15 dB for 16-PSK modulation. These values of E_b/N_0 ratios corresponds to a BER equal to $2.917 \cdot 10^{-4}$ (for QPSK transmission with 8 kb/s), $2.333 \cdot 10^{-4}$ (for QPSK transmission with 40 kb/s), $3.479 \cdot 10^{-4}$ (for 8-PSK transmission) and $6.354 \cdot 10^{-4}$ (for 16-PSK transmission), where the number of error bits is 140, 112, 167 and 305, respectively. These thresholds were determined empirically, running the application for all ten different image notifications, illustrated in Fig. 2. Due to a limited number of input data bits (480000) considered in our simulation setup, the estimation of BER can be considered accurate only for values greater than $2.083 \cdot 10^{-6}$ (1/480000).

B. TECHNIQUES TO MEASURE THE SNR BY USING A SPECTRUM ANALYZER FROM MATLAB-SIMULINK

In this section a new method to measure the signal-to-noise ratio of the received radiofrequency (RF) QPSK signal by using a spectrum analyzer from Matlab-Simulink is presented. This value is required to plot BER vs. E_b/N_0 ratio in order to characterize the QPSK transmission performance.

According to [34] and [35] since the spectrum analyzer performs the measurement of combined signal and noise power, and taking into account the logarithmic "decibel" scale, it is necessary to subtract the N from $(S+N)/N$ to obtain the true signal-to-noise ratio (SNR = S/N). This is especially useful for low SNR. If the transmission is performed without any error (or with a BER lower than an imposed value) for a very high number of transmitted bits (N_{bits}), then the signal power measured with the spectrum analyzer can be approximated to the power of the noiseless RF QPSK signal. Thus, for high value of the noiseless RF QPSK signal power (S) at the receiver stage, one can write:

$$S + N \cong S \tag{11}$$

The accuracy by which $(S+N)/N$ ratio is approximated with S/N can be calculated as follows:

$$\varepsilon = 100 \cdot \frac{(S+N)/N - S/N}{S/N} = 100 \cdot \frac{N}{S}(\%) \tag{12}$$

On the other hand, for a QPSK transmission, from (9), we obtain:

$$\frac{S}{N} = 2 \cdot \frac{E_b}{N_0} \tag{13}$$

By using (12) and (13), the error made in SNR approximation can be written as:

$$\varepsilon = 100 \cdot \frac{1}{2\left(E_b/N_0\right)} \tag{14}$$

TABLE 2. QPSK transmission parameters required to obtain different approximation errors of the SNR.

SNR error (ε) (%)	E_b/N_0 (dB)	S/N (dB)	S/N	BER	N_{bits}
4.75	10.23	13.23	21.04	$2.083 \cdot 10^{-6}$	$4.8 \cdot 10^{5}$
1	17	20	100	$6.759 \cdot 10^{-24}$	$1.48 \cdot 10^{23}$
0.5	20	23	199.53	$1.044 \cdot 10^{-45}$	$9.58 \cdot 10^{44}$

The average bit error probability for the QPSK modulation, considering Gray mapping and high E_b/N_0 is [27]:

$$\text{BER} \cong \frac{1}{2}\text{erfc}\left(\sqrt{\frac{E_b}{N_0}}\right) \tag{15}$$

From (14) we can easily determine the value of the E_b/N_0 ratio (denoted by $(E_b/N_0)_0$), for which the error ε is smaller than an imposed value (for example 1%). From (15) we can find the BERo value corresponding to the $(E_b/N_0)_0$ ratio.

Thus, by using this method, it is possible to find the BER value required to calculate the SNR with an error smaller than an imposed value. In Table 2 the transmission parameters (E_b/N_0, S/N ratios, BER and N_{bits}, where BER $= 1/N_{bits}$) required to obtain different approximation errors of the SNR are presented.

Simulations have been performed by using the circuits illustrated in Figs. 4 and 7, for each value of the E_b/N_0 ratio in the range 0 – 20 dB (at the emitter stage). The corresponding value of the SNR at the receiver stage has been calculated by using the following equation:

$$SNR = \frac{S_{meas}|_{\text{BER}\le\text{BERo}}}{S_{meas} - S_{meas}|_{\text{BER}\le\text{BERo}}} \tag{16}$$

where S_{meas} represents the combined signal and noise power, measured with the spectrum analyzer at the receiver stage and $S_{meas}|_{\text{BER}\le\text{BERo}}$ represents the power measured with the spectrum analyzer for a QPSK transmission having BER $\le$ BERo, thus meaning a simulation with a number of bits transmitted higher than $N_{bits} = 1/\text{BERo}$.

For a QPSK transmission with a very low bit error rate (corresponding to a very high number of bits transmitted), the signal power measured by the spectrum analyzer can be approximated with the noiseless RF QPSK signal power.

In Fig. 20 the BER vs. E_b/N_0 at the receiver stage plotted based on SNR values, obtained by measurement with different errors ($\varepsilon = 0$, 0.5% and 1%), according to (16), by using a spectrum analyzer from Matlab-Simulink is presented.

According to the simulations results illustrated in Table 2, for our case, when a number of $4.8 \cdot 10^5$ bits is transmitted, the approximation error of the SNR is 4.75%, a value that is too high to be accepted. On the other hand, in order to obtain a smaller error of the SNR approximation (lower than 1% or 0.5%), QPSK data transmissions with too many bits are required, being very difficult to implement practically.

In the experimental setup, the direct noise measurement (by using a transmission without QPSK signal) has given inaccurate results, since the measurement of the noise power levels with high accuracy requires high computation capabilities. In the following, a simpler noise power measurement by using a differential method is presented.

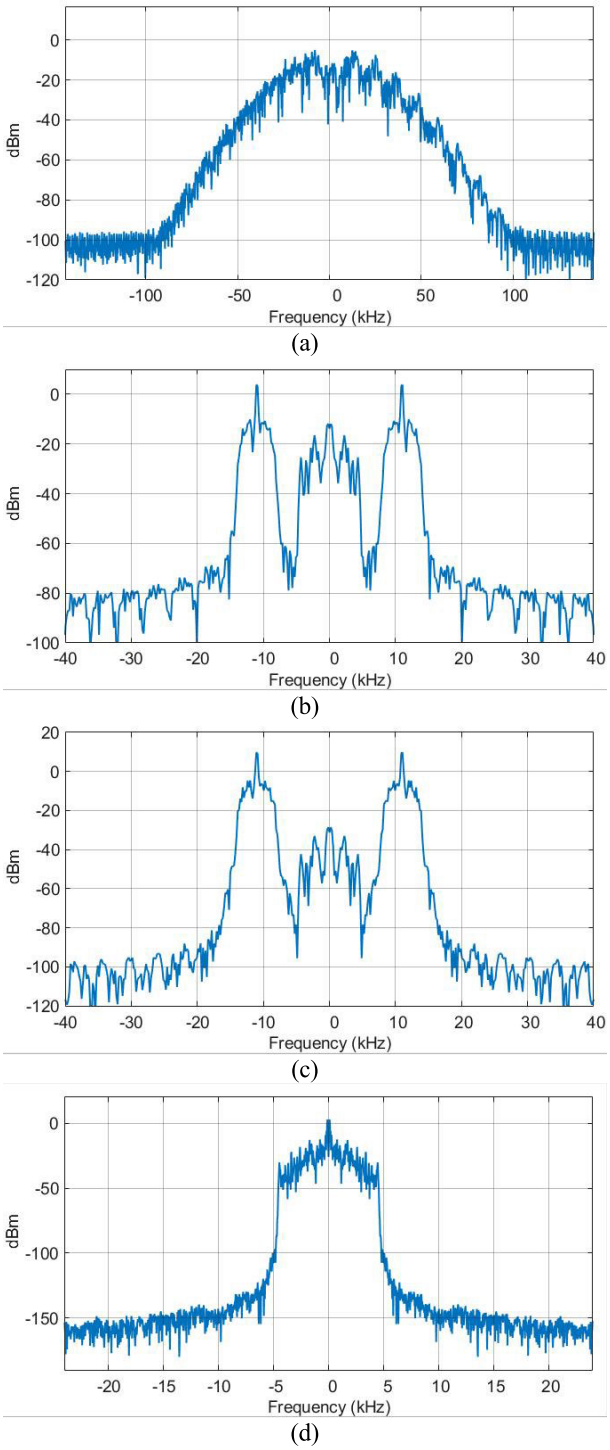

FIGURE 14. Mono FM radio transmission with QPSK data modulation and 8kb/s bit-rate for $E_b/N_0 = 11$dB: (a) Spectrum of the transmitted baseband FM signal ($2\pi K_{fm} = 4$Hz/V); (b) Spectrum of the transmitted customized baseband signal; (c) Spectrum of the received QPSK signal; (d) Spectrum of the received audio mono signal.

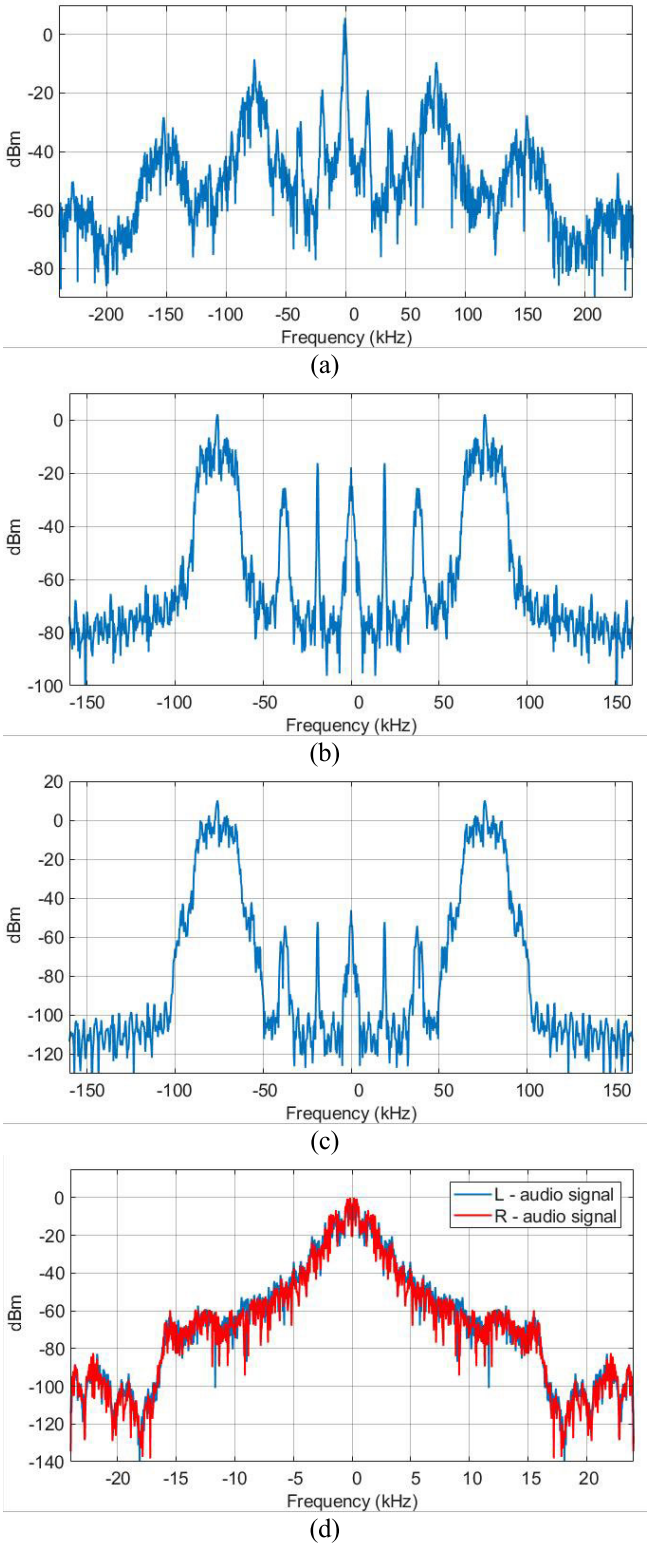

FIGURE 15. Stereo FM radio transmission with QPSK data modulation and 40kb/s bit-rate for $E_b/N_0 = 11$dB: (a) Spectrum of the transmitted baseband FM signal ($2\pi K_{fm} = 3$Hz/V); (b) Spectrum of the transmitted customized baseband signal; (c) Spectrum of the received QPSK signal; (d) Spectrum of the received audio stereo signal.

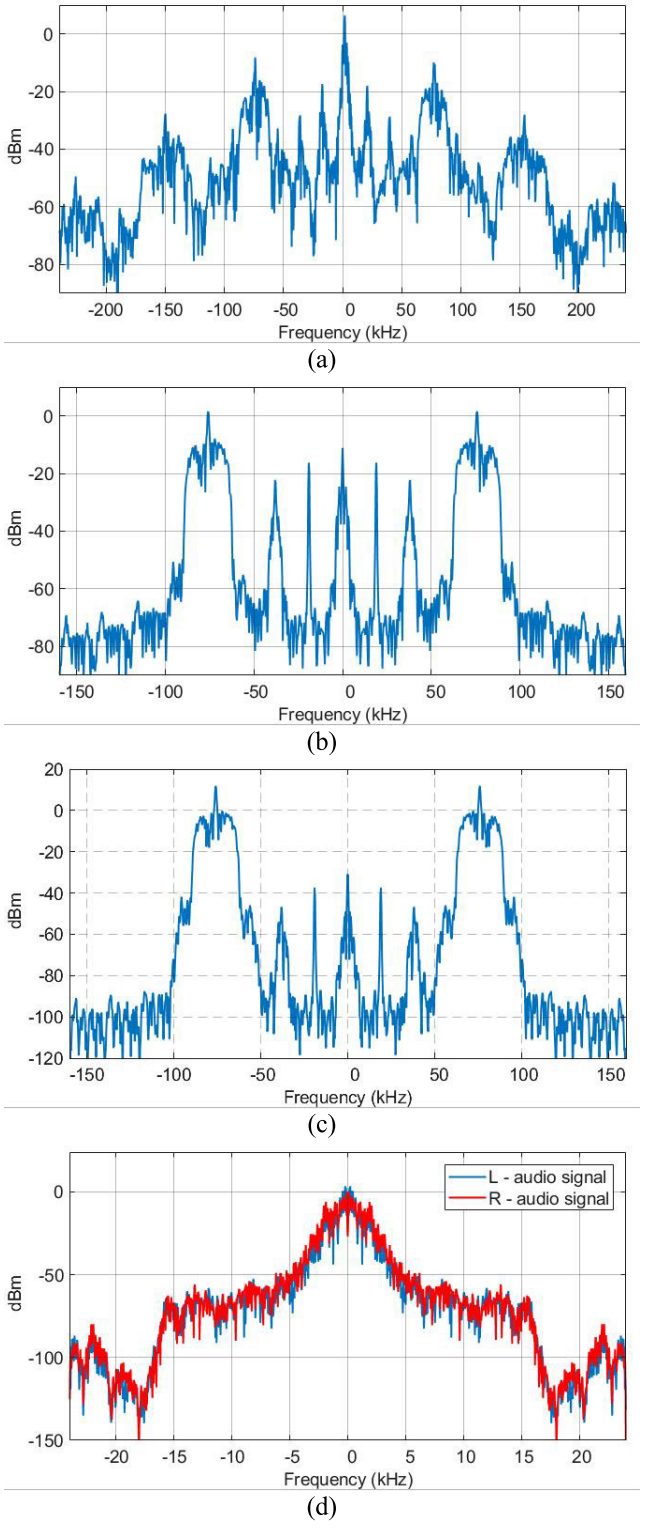

FIGURE 16. Stereo FM radio transmission with 8-PSK data modulation and 60kb/s bit-rate for $E_b/N_0 = 15$dB: (a) Spectrum of the transmitted baseband FM signal ($2\pi K_{fm} = 3$Hz/V); (b) Spectrum of the transmitted customized baseband signal; (c) Spectrum of the received 8-PSK signal; (d) Spectrum of the received audio stereo signal.

Because the customized baseband signal used by the transmitter is software generated, pairs of noiseless RF QPSK signals, that have a constant power ratio, can be easily generated. Thus, the signals measured by the spectrum analyzer

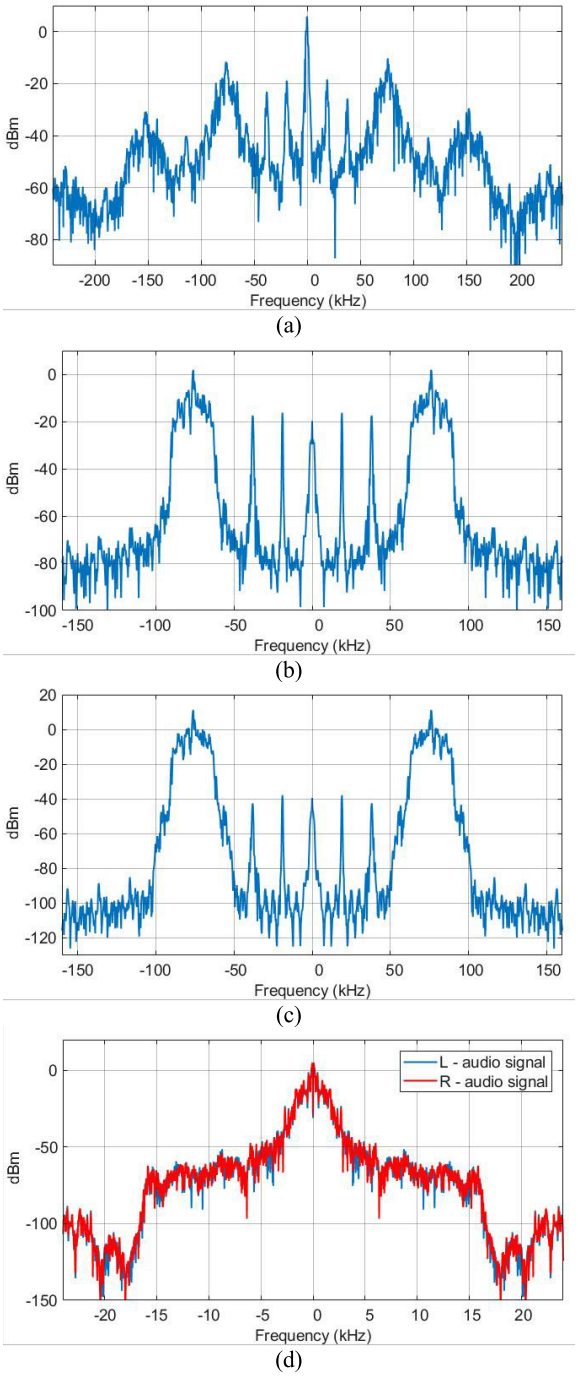

FIGURE 17. Stereo FM radio transmission with 16-PSK data modulation and 80kb/s bit-rate for $E_b/N_0 = 20$dB: (a) Spectrum of the transmitted baseband FM signal ($2\pi K_{fm} = 3$Hz/V); (b) Spectrum of the transmitted customized baseband signal; (c) Spectrum of the received 16-PSK signal; (d) Spectrum of the received audio stereo signal.

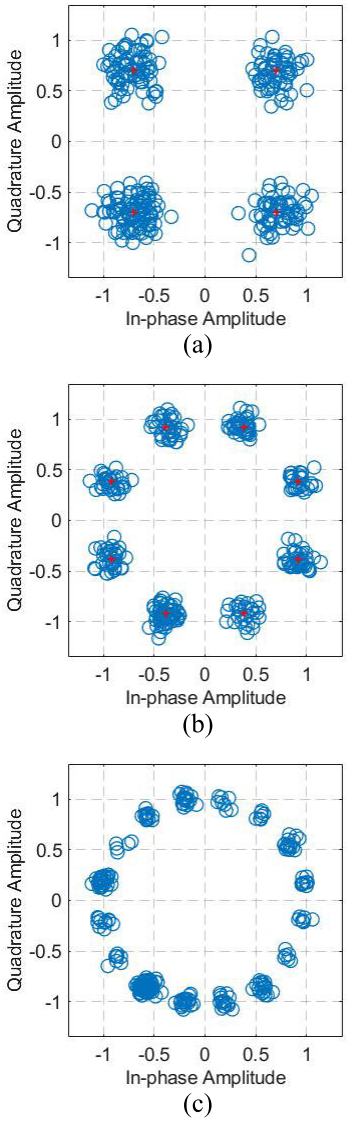

FIGURE 18. Constellation diagrams of all modulations used for digital transmission performed in the proposed application: (a) QPSK with 40kb/s bit-rate; (b) 8-PSK with 60 kb/s bit-rate; (c)16-PSK with 80 kb/s bit-rate.

are written:

$$\begin{cases} S_{meas1}|_{Se1=P} = S_{r1} + N \\ S_{meas2}|_{Se2=P+3\text{dB}} = S_{r2} + N \end{cases} \tag{17}$$

where S_{r1}, S_{r2} are two values of the received noiseless RF QPSK signal power, corresponding to a pair of transmitted RF QPSK signals having a constant power ratio, $S_{e2}/S_{e1} = 2$ (3 dB), N is the noise power introduced by the communication channel measured at the receiver stage, S_{meas1}, S_{meas2} represent the values of the combined signal and noise powers measured by the spectrum analyzer at the receiver stage, corresponding to the two noiseless RF QPSK signals, software generated at the emitted stage. For a noiseless transmission system, one can write:

$$S_{r2}/S_{r1} = S_{e2}/S_{e1} \tag{18}$$

Thus, from (17), and taking into consideration (18), the value of the noise power, expressed in Watts at the receiver stage is:

$$N = 2S_{meas1}|_{S_e=P} - S_{meas2}|_{S_e=P+3\text{dB}} \tag{19}$$

Next, the value of the SNR at the receiver stage is determined by using the following equation:

$$SNR = (S_{meas} - N)/N \tag{20}$$

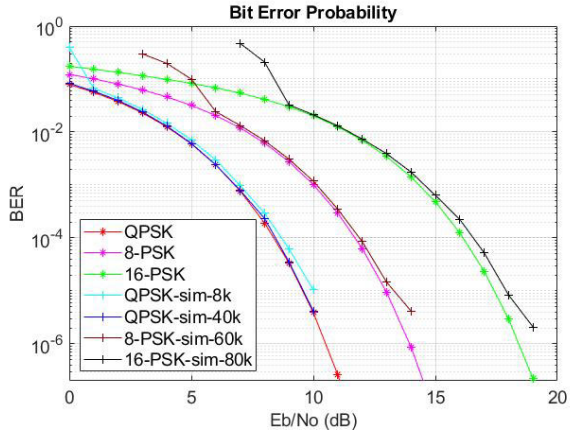

FIGURE 19. Bit error rate depending on E_b/N_0 for all digital transmissions analyzed in the proposed drivers' warning application and for ideal corresponding modulations (QPSK, 8-PSK, 16-PSK).

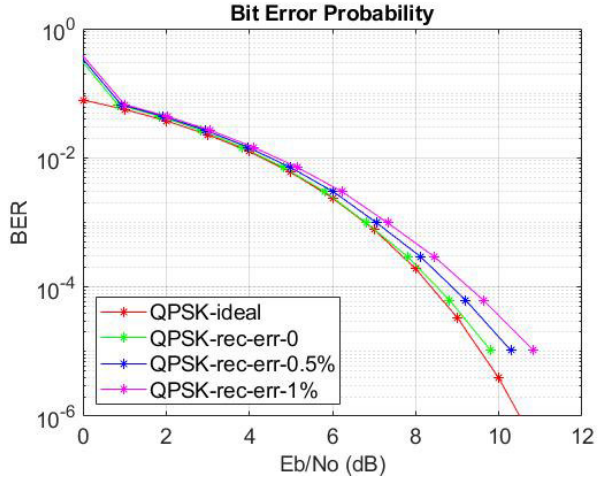

FIGURE 20. BER vs. E_b/N_0 at the receiver stage plotted based on SNR values obtained by measurement with different errors (0, 0.5% and 1%), by using a spectrum analyzer from Matlab-Simulink.

where S_{meas} represents the combined signal and noise power, measured with the spectrum analyzer at the receiver stage and N is the noise power, calculated with (19).

The noise power measurement accuracy based on (19) depends on the measurement accuracy of the combined signal and the noise power level. Since a high measurement accuracy requires high computing power for the spectrum analyzer, the noise power measurement was made for low values of the signal-to-noise ratio, where the noise level is significant. Thus, by using this method, very low values of the noise power can be measured accurately.

In order to demonstrate the proposed method validity, the same simulation setup as in previous case is used. A channel noise power, $N = 5.78 \cdot 10^{-6}$ W is considered and the values of the noiseless RF QPSK signal power (having a 3dB difference between them) are software generated at the emitter stage.

In Table 3 the noise power measurement by differential method using (19) for different emission powers, S_e, in the range −17–0 dBm is illustrated.

TABLE 3. Noise power measurement by differential method.

S_e (dBm)	S_{meas} (dBm)	N (dBm) calculated using (19)
0.9970	13.5830	-
-2.0030	10.6030	-7.9653
-5.0030	7.6440	-8.6480
-8.0030	4.7240	-9.1317
-11.0030	1.8790	-9.3882
-14.0030	-0.8273	-9.5172
-17.0030	-3.2960	-9.5948

TABLE 4. E_b/N_0 ratio calculation at the receiver stage and the BER values obtained by simulation.

S_e (dBm)	S_{meas} (dBm)	N (dBm)	E_b/N_0 calculated (dB)	BER (by simulation)
0.9970	13.5830	-9.5948	20.157	0
-2.0030	10.6030		17.156	0
-5.0030	7.6440		14.156	0
-8.0030	4.7240		11.155	0
-11.0030	1.8790		8.153	$1.771 \cdot 10^{-4}$
-14.0030	-0.8273		5.149	$5.298 \cdot 10^{-3}$
-17.0030	-3.2960		2.138	$6.474 \cdot 10^{-2}$

In Table 4 the E_b/N_0 ratio calculation at the receiver stage is performed for different emission power in the range −17–0 dBm and for the most accurate noise power measurement presented in Table 3 ($N = -9.59$ dBm). The BER values presented is Table 4 have been obtained by simulation, considering a number of $4.8 \cdot 10^5$ input bits transmitted.

In Fig. 21 the BER vs. E_b/N_0 at the receiver stage plotted based on SNR values obtained by measurement with the differential method, by using a spectrum analyzer from Matlab-Simulink for different values of the determined noise power (illustrated in Table 3) is presented.

Therefore, according to the simulation results illustrated in Fig. 21, the most accurate value of the noise power, N, is the one resulting from the last measurement illustrated in Table 3 ($N = -9.59$ dBm), which corresponds to the smallest measured value of the $S + N$ signal, where the noise has a non-negligible value. In our case, this recording corresponds to the lowest measured value $S + N$, which still allows the reception of the image, although with a very low quality.

This differential method of noise power measurement is employed in the practical experiments, presented below, to calculate the SNR, used in order to plot BER vs. E_b/N_0 ratio at the receiver stage.

C. EXPERIMENTAL RESULTS

In order to validate our proposed approach and the simulation results, an experimental setup was built for the case of mono FM transmission. The general architecture of the FM broadcasting of a composite signal formed by the audio mono component, the pictogram sent by using QPSK modulation, and the RDS component is given in Fig. 22.

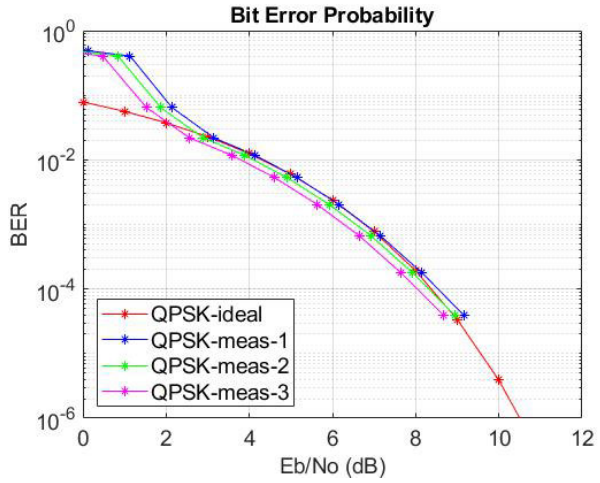

FIGURE 21. BER vs. E_b/N_0 at the receiver stage plotted based on SNR values obtained by measurement with the differential method, by using a spectrum analyzer from Matlab-Simulink for different values of the determined noise power: $N = -9.59$ dBm (blue curve); $N = -9.38$ dBm (green curve); $N = -9.13$ dBm (magenta curve).

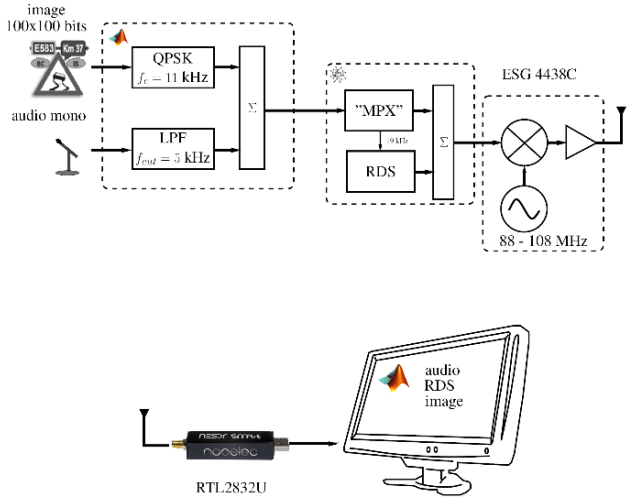

FIGURE 22. Synoptic of the experimental setup.

A custom ''MPX like'' signal is built by Matlab-Simulink program. This composite signal contains the audio and the QPSK signals and it is played by a Smartphone.

The RDS encoder combines the custom ''MPX like'' signal with the RDS one to generate the customized baseband signal.

The encoder is built by the authors by using the shelf components.

The obtained waveform modulates in frequency an RF carrier chosen outside the European FM band (88 - 108 MHz). This FM modulation is performed by using an ESG 4438C vector signal generator.

Fig. 23 presents a photograph of the experimental setup. In this picture (a) is the laptop running Matlab/Simulink used in order to build the baseband composite signals and to process (demodulate) the received signal flow from the RTL–SDR receiver, (b) is the ESG 4438C arbitrary waveform generator which performs the FM modulation, (c) is the RDS

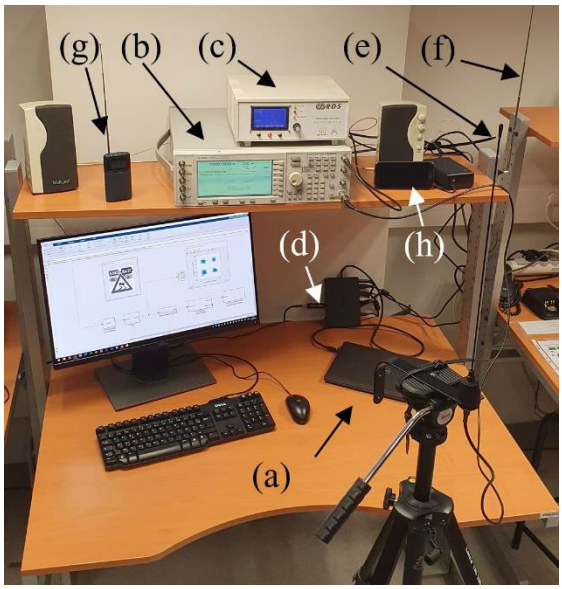

FIGURE 23. Photograph of the experimental setup.

encoder, (d) is the RTL2832U dongle, USB connected to the laptop and used as radio receiver; the emitting (e) and the receiver antennas (f) are classical omnidirectional ones; they have been placed at two meters separation; this distance was chosen in order to have a good signal-to-noise ratio level for the RF signal; the radio receiver (g) is used in order to ''sniff'' the emitted signal and to test if it is compliant to a classical commercial solution; (h) is a Smartphone.

The waveforms containing the audio mono component (up to 5 kHz) and the QPSK signal onto 11 kHz carrier were built in Matlab with a sampling frequency of 288 kHz and played back as audio files by a Smartphone (h). In the experiments presented here, no pre-emphasis/de-emphasis filters were employed.

The main concern was to characterize the transmission of the pictogram through the QPSK modulation. This transmission is performed at a data rate of 8 kbit/sec and modulating a subcarrier at 11 kHz. The RF carrier was chosen at 109 MHz, in order to avoid the interference with the commercial radio stations. The emitted power level was 0 dBm and a frequency deviation of +/−75 kHz, identical to the commercial standard, was configured.

At the receiver side, an RTL-SDR 2832U device coupled with Matlab-Simulink software is used. This dongle performs a direct conversion (0 IF) of the received RF signal. The sampling frequency of the baseband signal was chosen identical to the one at the emission, i. e. 288 kHz. Moreover, a fixed low noise amplifier (LNA) gain level (30 dB) was setup.

The circuits illustrated at system level in Figs. 4 and 7, including blocks from the ''RTL-SDR book library'' [15], were used to encode and to decode the various gray scaled pictograms (100 × 100 bits) and to configure the RTL-SDR 2832U dongle's parameters.

From our application point of view (driver's warning notification), the RDS component may transmit brief information

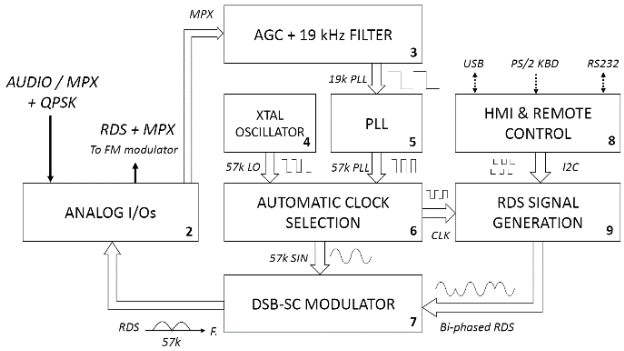

FIGURE 24. Internal architecture of the RDS encoder.

about traffic events, destinated to cars without a Tablet PC and to assure the full compatibility of the proposed system with the existing car park.

The internal architecture of the RDS encoder is presented in Fig. 24. The composite signal at the encoder's input is filtered in order to obtain the pilot signal at 19 kHz. Then, an amplitude adjustment is performed by an automated gain control circuit which delivers the input signal of a PLL. The PLL locks on the 19 kHz signal and delivers the carrier frequency for the RDS encoder (57 kHz).

The baseband RDS signal is generated by using a microcontroller (ATmega16) and an R-2R digital to analog converter (D/AC) followed by a restitution filter.

The baseband RDS signal data rate is 1187.5 Hz (= 57 kHz /48) and the D/AC's output is actualized eight times each RDS symbol time ($TD/AC = 105.26\ \mu s$). The microcontroller is programmed via an I2C interface with the RDS services (Program Service, Radio Text, Alternative Frequencies, Traffic Announcement, etc.).

The waveforms at the output of the R-2R D/AC (top) and at the output of the restitution filter are presented in Fig. 25.

As mentioned, the 57 kHz subcarrier for the RDS signals is delivered by a CD4046 PLL working as a frequency multiplier (x3). In order to be independent to the MPX signal's amplitude, an automatic gain control stage using a JFET transistor working as a controlled resistance is used. This stage is between the MPX encoder and the PLL.

The JFET transistor varies its resistance inversely proportional to the amplifier's output and in this way a regulation of the 19 kHz signal amplitude is performed. The 57 kHz subcarrier is modulated by the base-band RDS signal by using a SA602 Gilbert cell. A double-sideband suppressed-carrier (DSB-SC) amplitude modulation is performed here. The measured time domain waveform (up) together with the corresponding spectrum (bottom) are presented in Fig. 26.

At the receiver side, an RTL-SDR dongle, USB connected at a PC running Matlab-Simulink environment are employed.

In order to be used for digital communications, the RTL-SDR dongle requires a calibration procedure [15], which determines the offset between the carrier frequency generated by its internal PLL circuitry and the carrier frequency of the emitted signal (the one generated by the ESG 4438C).

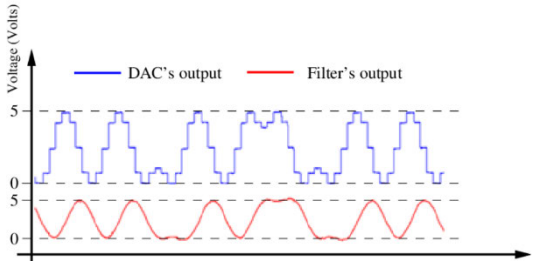

FIGURE 25. Measured waveforms of the digital to analog converter (top) and of the "baseband" RDS signal.

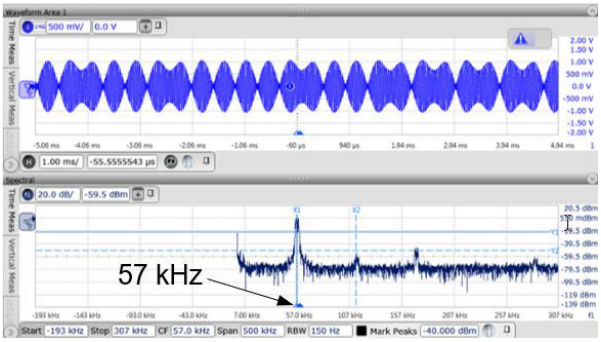

FIGURE 26. Measurement of the RDS signal: time domain waveform (top) and the corresponding spectrum (bottom).

As in the simulation framework, the FM demodulation was performed by a Complex Delay Line Frequency Discriminator, as shown in Section 2.

The processing of the received signal was performed offline on recordings lasting approximately one minute.

Fig. 27 presents the spectrum of the received signal, after the demodulator for an emitted power level of the QPSK signal equal to 3 dBm. Fig. 28 presents the received QPSK constellation.

The three components of the received composite signal in Fig. 27 (the audio mono, the QPSK signal and the RDS one) have been separated by using the proposed software-defined receiver illustrated in Fig. 7.

For this power of the emitted signal, the data transmission is performed without any errors.

The RDS signal was also decoded without errors, whenever the power level of the emitted QPSK signal was setup, thus proving the good separation between the three components of the composite signal.

In this case, the playback of the audio part of the received signal was of an acceptable quality, even if the sound corresponding to the QPSK signal was audible.

As a comparison with the previous results, Figs. 29 and 30 present the spectrum of the composite signal after the FM demodulation and the IQ constellation diagram of the QPSK signal having a low SNR value, respectively.

In this case, the emitted power level was −16 dBm. As can be remarked, the constellation is spreaded, the four states of this modulation being mixed up.

In Fig. 31, the interface of the RDS/RBDS receiver proposed by Matlab-Simulink is presented. The RDS component

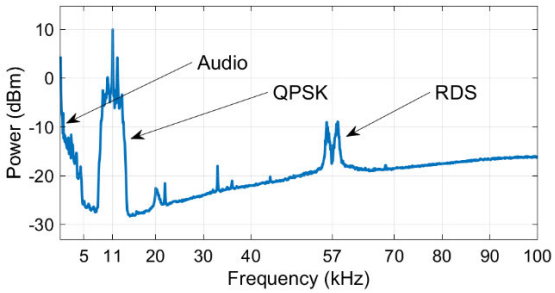

FIGURE 27. Received composite signal (audio + QPSK + RDS) after the FM demodulation. The QPSK emitted power level is 3 dBm.

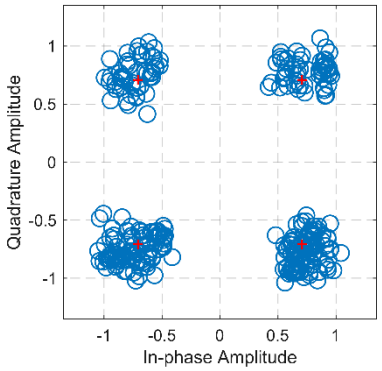

FIGURE 28. The constellation of the received QPSK signal when the corresponding emitted power level is 3 dBm and the received power level is 15.5 dBm.

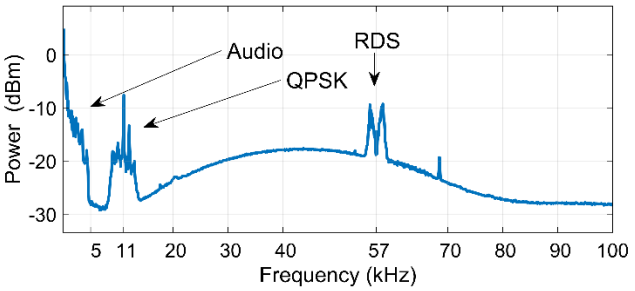

FIGURE 29. Received composite signal (audio + QPSK + RDS) after the FM demodulation. The QPSK emitted power level is −16 dBm.

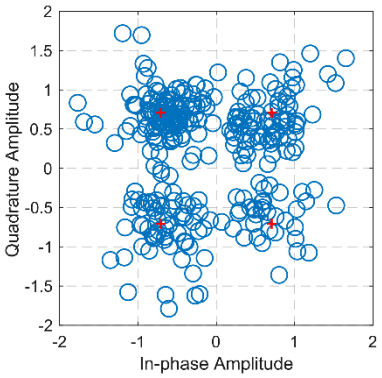

FIGURE 30. The constellation of the received QPSK signal when the corresponding emitted power level is −16 dBm and the received power level is approximatively 0 dBm.

of the transmitted signal is decoded properly, the radio text message setup at the RDS encoder, *"INSA Lyon, France & ETTI Iasi, Romania"*, being displayed.

Fig. 32 shows a photograph of the FM radio's LCD display featuring the same received message.

This demonstrates the full compatibility of the proposed approach with the classical FM broadcasting infrastructure.

The setup previously described allowed the extraction of the bit error rate as a function of the E_b/N_0 ratio. At the transmitter, the QPSK signal was software configured in order to have different power levels, while the audio and the RDS signals were kept at the same level, specific to FM transmission standards [36].

The results of the measurement campaign are presented in Table 5. Some examples of received images for different values of emitted power levels are presented in Fig. 33.

For an emitted power level (S_e) of the RF QPSK signal equal or lower than −16 dBm (which corresponds to a received power of approximately 0 dBm), the frame synchronization was not possible anymore. Moreover, the symbol synchronization is lost during the transmission.

For an emitted power equal or higher than −9 dBm (which corresponds to a received power of 6.29 dBm), there was no error transmission for an approximative number of transmitted bits equal to $4.8 \cdot 10^5$, which corresponds to a transmission of 61 seconds and to a transmission of four pictograms.

According to the experimental results, for transmission power of the RF QPSK signal in the range illustrated

TABLE 5. Measured QPSK transmission parameters.

S_e (dBm)	S_r (dBm)	N (dBm)	No. error bits	E_b/N_0 (dB)	Total bits	Measured BER
-9	6.294	-9.716	0	12.900	476801	0
-10	5.508		1	12.092	459577	$2.176 \cdot 10^{-6}$
-11	4.638		2	11.192	474341	$4.216 \cdot 10^{-6}$
-12	3.747		1	10.263	475037	$2.105 \cdot 10^{-6}$
-13	2.873		42	9.343	463645	$9.059 \cdot 10^{-5}$
-14	1.805		542	8.204	474285	$1.143 \cdot 10^{-3}$
-15	1.251		5323	7.605	463656	$1.148 \cdot 10^{-2}$
-16	0.068		2499	6.302	469055	$5.328 \cdot 10^{-3}$

in Table 5 (−9 dBm, −16 dBm), the quality of the audio signal is not impacted by the QPSK signal.

The received signal's power level (S_r) was measured by using the Simulink's spectrum analyzer.

The noise power (N) has been determined by using the differential method proposed in previous Subsection. As stated, the measured value of the noise power depends on the accuracy of the combined signal and noise power value measurement with a software spectrum analyzer. In order to avoid a high processing power and to obtain a relatively good accuracy of the spectrum analyzer, the noise power measurement is performed for low SNR.

Moreover, in order to increase the noise measurement accuracy, the average between two most representative noise

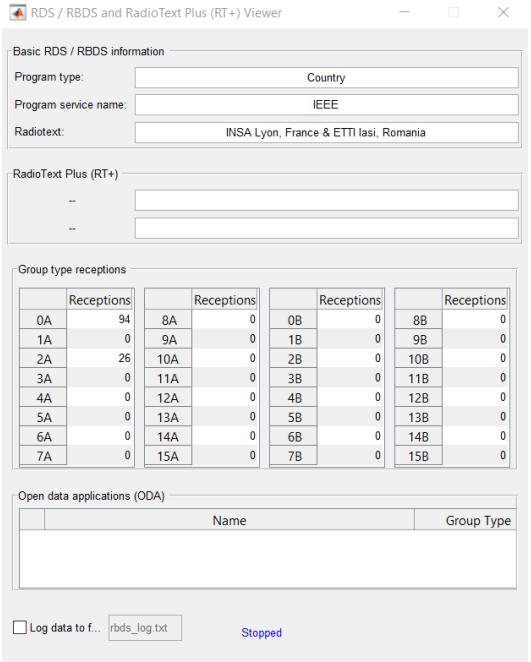

FIGURE 31. Message contained in the RDS signal and decoded by Matlab/Simulink RDS/RBDS tool.

FIGURE 32. RDS message decoded by a commercial FM radio receiver.

FIGURE 33. Examples of received pictograms for different levels of emitted power levels: (a) $S_e = -9$ dBm; BER = 0; (b) $S_e = -14$ dBm; BER = $1.143 \cdot 10^{-3}$; (c) $S_e = -16$ dBm; BER = $5.328 \cdot 10^{-3}$.

values was calculated. Indeed, the noise power was calculated from (19), by using two values of the P parameter: -16 dBm and -14 dBm. These values were considered the most significant ones, because they are corresponding to the lowest exploitable SNR. The measurement performed for an emitted power of -15 dBm was out of range. Experimental results demonstrated that the noise level may vary in a random way due to the fact that a symbol synchronization loop is not implemented yet. Even in this condition, the experimental

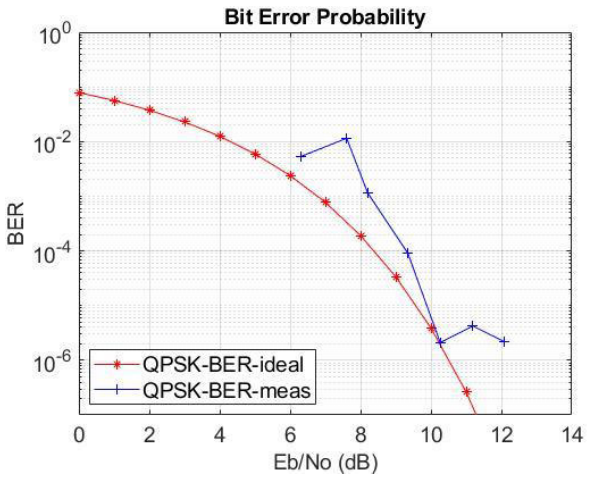

FIGURE 34. The experimental BER extraction as function of the E_b/N_0 ratio compared to the ideal BER for an AWGN communication channel.

results show a relatively good agreement between the calculated BER values and the theoretical ones.

Taking into account all these considerations, the average value of the noise power level used in order to determine the E_b/N_0 ratios is equal to -9.716 dBm.

In Fig. 34 are plotted BER values obtained experimentally depending on the E_b/N_0 ratio (presented in Table 5). For comparison, on the same figure, the ideal theoretical values of BER vs. E_b/N_0 ratio for an AWGN communication channel are also represented. According to the obtained results, the measured BER variation has a certain coherence with respect to the theory. From the experimental results, illustrated in Fig. 34, we can remark that the minimum calculated value of BER is equal to $2.1 \cdot 10^{-6}$, representing the maximum accuracy value in BER calculation, obtained for a number of the $4.8 \cdot 10^5$ transmitted bits.

According to the simulation results, illustrated in Section 3, the received image notification has been considered of high quality for a BER lower than $2.917 \cdot 10^{-4}$ (which corresponds to a $E_b/N_0 = 8$ dB). In the case of the experimental setup this value of BER is difficult to be determined exactly, but, according to the experimental measurements, it corresponds to a power of the transmitted QPSK signal between -14 dBm and -13 dBm.

This study allowed us to choose properly the QPSK signal's power level compared to audio and RDS signal levels, so that making possible to receive image notifications.

According to the results obtained experimentally, the acceptable power level range of the emitted QPSK signal, required to receive properly the image notifications together with the usual radio broadcasting, is between -16 dBm and -9 dBm; this corresponds to a power level range of the received QPSK signal between 0 dBm and 6.29 dBm.

IV. CONCLUSION

In this paper a new drivers' warning application has been proposed. The application uses an FM radio infrastructure to

transmit real-time image notifications in order to warn drivers about an important traffic event.

The reception of image notifications is performed together with the usual FM radio broadcasting by using an RTL-SDR dongle, USB connected to a car device running the proposed software-defined radio receiver application. The bit-rate of the image notifications is 8 kb/s for QPSK data transmission on the mono FM broadcasting and 40 kb/s, 60 kb/s, 80 kb/s for QPSK, 8-PSK, 16-PSK data transmission, respectively, on the stereo FM broadcasting.

In this paper, different methods for the experimental measurement of the SNR and E_b/N_0 ratio by using a software spectrum analyzer has been proposed. These methods allow decreasing the exigence in terms of computational capabilities.

The performance of the proposed application has been analyzed by plotting BER vs. E_b/N_0 ratio (determined experimentally and by simulation) for different FM transmission scenarios.

According to simulation results, the image notifications are of high quality for the proposed drivers' warning application for E_b/N_0 ratios higher than: 8 dB for QPSK modulation implemented in both mono and stereo FM transmission; 11 dB for 8-PSK modulation and 15 dB for 16-PSK modulation.

The experimentally obtained results on the mono FM radio transmission show that the received image notification is of high quality for a transmitted signal power of the RF QPSK signal higher than −12 dBm. This value of the transmitted signal power determines a E_b/N_0 ratio at the receiver stage of approximatively 10 dBm. The small difference from the simulated transmission performed on an AWGN communication channel is due to noise introduced by the RTL-SDR device and wireless transmission impairments.

The proposed drivers' warning application has the following clear advantages compared to other similar ones: (1) increase drivers' safety by warning them of imminent dangers that may occur in traffic: traffic jams, wet road, works on public roads, rugged roads, impassable roads, car accidents, worsening weather, bypassing certain obstacles in traffic, landslides, police control; (2) the proposed application is inexpensive and easy to implement because it uses an existing and very widespread radio FM infrastructure; the proposed system includes an existing FM broadcasting station - for transmission and a cheap RTL - SDR device, attached to a Tablet PC (present in most of the cars today) and connected to the car aerial - for receiving; this significantly lowers the cost price of the system; (3) the FM radio ensures a very good quality of the received signal and good coverage of a large geographical area; (4) the application provides reliable data transmission at constant rate even in noisy conditions; (5) the application allows simultaneous reception in real-time of the image notifications together with the usual FM radio broadcasting; (6) image notifications are easy to receive and understand by drivers without distracting them from driving and do not require the interruption of the radio station broadcasting; (7) signaling dangerous situations in traffic is made by the road authorities and not by other traffic participants, as in the case of other applications; (8) the proposed application does not require an Internet connection, which may be poor in certain geographical areas along public roads; (9) the proposed system is flexible, easily adapts to the transmission of any type of image notification, and can be easily installed and used by drivers; (10) the proposed application can also be used in cars that do not have a Tablet PC, by sending the warning notification in a simplified form, as a text message on the RDS signal of the FM broadcasting.

Future work may be dedicated to increase the data rate and the robustness of data transmission by introducing a symbol synchronization loop and by using a certain type of codding (JPEG, PNG, GIF). In order to overcome the multipath interference, which is an important issue for mobile reception, error correction coding may also be introduced.

REFERENCES

[1] Road Safety Facts & Figures. (2020). *European Commission*. Accessed: Dec. 7, 2020. [Online]. Available: https://ec.europa.eu/transport/road_safety/road-safety-facts-figures-1_en

[2] Annual Accident Report. (2018). *European Road Safety Observatory*. Accessed: Dec. 7, 2020. [Online]. Available: www.erso.eu

[3] Strategic Action Plan on Road Safety, Annex 1. (May 17, 2018) *European Commission*. Accessed: Accessed: Dec. 7, 2020. [Online]. Available: https://eur-lex.europa.eu/resource.html?uri=cellar%3A0e8b694e-59b5-11e8-ab41-01aa75ed71a1.0003.02/DOC_2&format=PDF

[4] (Jun. 19, 2019). *Vision Zero*. Accessed: Dec. 7, 2020. [Online]. Available: https://ec.europa.eu/transport/road_safety/sites/roadsafety/files/move-2019-01178-01-00-en-tra-00_3.pdf

[5] (2016). *Guide to Car Safety Features*. Accessed: Dec. 7, 2020. [Online]. Available: https://www.consumerreports.org/cro/2012/04/guide-to-safety-features/index.htm

[6] J.-P. Kreiss, L. Schüler, and K. Langwieder, "The effectiveness of primary safety features in passenger cars in Germany," in *Proc. 19th ESV Conf.*, 2005, p. 145.

[7] F. Jiménez, J. E. Naranjo, J. J. Anaya, F. García, A. Ponz, and J. M. Armingol, "Advanced driver assistance system for road environments to improve safety and efficiency," *Transp. Res. Procedia*, vol. 14, pp. 2245–2254, Dec. 2016, doi: 10.1016/j.trpro.2016.05.240.

[8] R. Grace, V. E. Byrne, D. M. Bierman, J.-M. Legrand, D. Gricourt, B. K. Davis, J. J. Staszewski, and B. Carnahan, "A drowsy driver detection system for heavy vehicles," in *Proc. 17th DASC. AIAA/IEEE/SAE. Digit. Avionics Syst. Conf.*, vol. 2, Dec. 1998, pp. 1–8, doi: 10.1109/DASC.1998.739878.

[9] F. Friedrichs and B. Yang, "Drowsiness monitoring by steering and lane data based features under real driving conditions," in *Proc. 18th Eur. Signal Process. Conf.*, vol. 2010, pp. 209–213.

[10] A. Kade, A. W. Finch, and K. S. Lybecker. (Apr. 2007). *Vehicular Lane Monitoring System Utilizing Front and Rear Cameras*. [Online]. Available: https://www.freepatentsonline.com/y2007/0091173.html

[11] T. Chia Chieh, M. M. Mustafa, A. Hussain, S. F. Hendi, and B. Y. Majlis, "Development of vehicle driver drowsiness detection system using electrooculogram (EOG)," in *Proc. 1st Int. Conf. Comput., Commun., Signal Process. Special Track Biomed. Eng.*, Nov. 2005, pp. 165–168, doi: 10.1109/CCSP.2005.4977181.

[12] B. Alshaqaqi, A. S. Baquhaizel, M. E. A. Ouis, M. Boumehed, A. Ouamri, and M. Keche, "Driver drowsiness detection system," in *Proc. 8th Int. Workshop Syst., Signal Process. their Appl. (WoSSPA)*, May 2013, pp. 151–155, doi: 10.1109/WoSSPA.2013.6602353.

[13] S. Singh and N. P. Papanikolopoulos, "Monitoring driver fatigue using facial analysis techniques," in *Proc. 199 IEEE/IEEJ/JSAI Int. Conf. Intell. Transp. Syst.*, 1999, pp. 314–318, doi: 10.1109/ITSC.1999.821073.

[14] B. Warwick, N. Symons, X. Chen, and K. Xiong, "Detecting driver drowsiness using wireless wearables," in *Proc. IEEE 12th Int. Conf. Mobile Ad Hoc Sensor Syst.*, Oct. 2015, pp. 585–588, doi: 10.1109/MASS.2015.22.

[15] R. W. Stewart, K. W. Barlee, and D. S. Atkinson, *Software Defined Radio Using MATLAB & Simulink and the RTL-SDR*. New York, NY, USA: Academic, 2015.
[16] A. L. Perrone and G. Basti, "RF video transmission," in *Proc. Int. Joint Conf. Neural Netw.*, 2002, pp. 2219–2224.
[17] F. Rochim and others, "SCA system (subsidiary communications authorization) implementation of text transmission on broadcasting system," in *Proc. ICICI*, 2005, pp. 4–5.
[18] C. C. Do and H. H. Szu, "Video compression transmission via FM radio," in *Proc. Wavelet Appl.*, Mar. 2001, pp. 455–464.
[19] M. Mitchum, "Transmission of compressed-video signals via FM subsidiary communications authorization," *IEEE Trans. Broadcast.*, vols. B-20, no. 4, pp. 77–82, Dec. 1974, doi: 10.1109/TBC.1974.266146.
[20] A. Rembovsky, A. Ashikhmin, V. Kozmin, and S. Smolskiy, *Radio Monitoring, Problems, Methods and Equipment* (Lecture Notes in Electrical Engineering). Cham, Switzerland: Springer, 2009.
[21] M. Takada, T. Kuroda, and O. Yamada, "FM multiplex broadcasting system 'DARC"," in *Proc. Vehicle Navigat. Inf. Syst. Conf.*, 1994, pp. 111–116, doi: 10.1109/VNIS.1994.396754.
[22] (Oct. 22, 1988). *Federal Communications Commission*. Accessed: Dec. 7, 2020. [Online]. Available: https://www.fcc.gov/media/radio/subcarriers-sca
[23] P. B. Kenington, *RF and Baseband Techniques for Software Defined Radio*. Norwood, MA, USA: Artech House, 2005.
[24] C. R. Johnson, Jr., W. A. Sethares, and A. G. Klein, *Software Receiver Design: Build Your Own Digital Communication System in Five Easy Steps*, Cambridge, U.K.: Cambridge Univ. Press, 2011.
[25] T. J. Rouphael, *RF and Digital Signal Processing for Software-Defined Radio: A Multi-Standard Multi-Mode Approach*. Burlington, MA, USA: Newnes, 2009.
[26] A. M. Wyglinski, R. Getz, T. Collins, and D. Pu, *Software-Defined Radio for Engineers*. Norwood, MA, USA: Artech House, 2018.
[27] D. A. Guimaraes, *Digital Transmission: A Simulation-Aided Introduction With Vissim/Comm*. Cham, Switzerland: Springer, 2010.
[28] L. W. Couch, *Digital & Analog Communication Systems*, 8th ed. Upper Saddle River, NJ, USA: Prentice-Hall, 2013.
[29] Ali Grami, *Introduction to Digital Communications*, Amsterdam, The Netherlands: Elsevier, 2016.
[30] S. S. Haykin, *Digital communications*. New York, NY, USA: Wiley, 1988.
[31] P. Davies and G. Klein, "RDS-alert-advice and problem location for European road traffic," in *Proc. Drive Conf.*, vol. 1, 1991, pp. 482–503.
[32] F. Ling, *Synchronization in Digital Communication Systems*. Cambridge, U.K.: Cambridge Univ. Press, 2017.
[33] H. Osborne, "A generalized 'Polarity-type' costas loop for tracking MPSK signals," *IEEE Trans. Commun.*, vol. 30, no. 10, pp. 2289–2296, Oct. 1982, doi: 10.1109/TCOM.1982.1095399.
[34] D. A. Hill and D. P. Haworth, "Accurate measurement of low signal-to-noise ratios using a superheterodyne spectrum analyzer," *IEEE Trans. Instrum. Meas.*, vol. 39, no. 2, pp. 432–435, Apr. 1990, doi: 10.1109/19.52530.
[35] (1979). *Spectrum Analysis—Noise Measurements, Hewlett-Packard Application Note 150-4*. Accessed: Dec. 7, 2020. [Online]. Available: http://www.hpmemoryproject.org/an/pdf/an_150-4.pdf
[36] *Transmission Standards for FM Sound Broadcasting at VHF*, document ITU Rec. BS.450, 2010. Accessed: Dec. 7, 2020. [Online]. Available: https://www.itu.int/rec/R-REC-BS.450/en

RADU GABRIEL BOZOMITU (Member, IEEE) was born in Iaşi, Romania, in 1971. He received the degree in electronic engineering and communications, the master's degree in the field of digital radio-communications, and the Ph.D. degree in electronics and telecommunications from the Faculty of Electronics, Telecommunications and Information Technology, Gheorghe Asachi Technical University of Iaşi, in 1995, 1996, and 2005, respectively. In 1998, he joined the Department of Telecommunications and Informational Technologies, Faculty of Electronics, Telecommunications and Information Technology, Gheorghe Asachi Technical University of Iasi. He received the title of Professor, in 2017. In 2020, he became the Vice-Dean of the Faculty. He taught courses at Gheorghe Asachi Technical University of Iasi, such as radio communications, VLSI implementation of the radiofrequency circuits, advanced radio communications, and software-defined radio. He is the author of five books and more than 115 articles. His research interests include radio communications, analog integrated circuit design, signal processing, and assistive technology.

FLORIN DORU HUTU (Senior Member, IEEE) was born in Iasi, Romania, in 1979. He received the engineer degree in electronics and telecommunications and the master's degree in digital radio-communications from the Faculty of Electronics, Telecommunications and Information Technology, Gheorghe Asachi Technical University of Iasi, in 2003 and 2004, respectively, and the Ph.D. degree in automatic control from the University of Poitiers, France, in 2007.

After two years of a Postdoctoral position with XLIM Laboratory, in September 2010, he became an Associate Professor with INSA Lyon, France. He joined the INSA Lyon's Electrical Engineering Department and the INRIA's Socrate Team of CITI Laboratory. He is the author of more than 70 national and international scientific articles. His research interests include energy efficient radio communications (wake-up radio, energy harvesting and wireless power transfer) and RFID technologies. He is also involved in the design of software defined radio architectures for the IoT.

NICOLAS DE PINHO FERREIRA (Graduate Student Member, IEEE) was born in Istres, France, in 1995. He received the Diploma degree in electrical engineering from the National Institute of Applied Science, Lyon, in 2018. He is currently pursuing the Ph.D. degree with the Lyon Nanotechnologies Institutes. His research interests include wearable sensors, physiological measurements, wireless body area networks, analog electronic design, and wireless transmissions.